

Spaceport America Cup – Project Raziel

Team 35 Project Technical Report for the 2017 IREC

Andrew C. Adams¹ and Andrew E. Kurtz²
Massachusetts Institute of Technology, Cambridge, MA, 02139

The MIT Rocket Team submits Project Raziel as an entrant in the 2017 Spaceport America Cup 10k – COTS – All Propulsion Types category. Raziel utilizes an Aerotech M2500-T motor and adjustable ballast to boost it to the desired apogee of 10,000 feet. The rocket’s structure consists of a custom airframe and nosecone fabricated using fiberglass and epoxy. The avionics for Project Raziel includes a custom flight computer, as well as a commercial Telemetrum. Recovery of the rocket utilizes a dual separation, dual deploy scheme with black powder charges and custom designed parachutes. The onboard payload consists of a rover, deployed upon landing, that utilizes an x-ray fluorescence sensor to determine soil composition of the landing site. Thorough analyses and tests have been conducted to ensure the safety and reliability of Project Raziel.

Nomenclature

A	=	area
C_D	=	coefficient of drag
D	=	drag
g	=	gravitational acceleration
m	=	mass
ρ	=	density of air
V	=	speed

I. Introduction

The MIT Rocket Team (hereafter, the Team) is a well-established student group open to the MIT community. The Team has students from several majors at MIT, and is currently unaffiliated with any senior design or capstone class. The Team receives funding from the MIT AeroAstro department, the MIT Edgerton Center, and various corporate sponsors.

Project Raziel is the Team’s entry into the 10,000 foot, COTS Solid category. In order to tackle the various tasks surrounding the development of Raziel, the Team is split into six subteams based on the different subsystems of the rocket. The six subteams include propulsion, structures, avionics, recovery, payload, and ground support equipment. Each subteam has a leader who is responsible for delegating tasks related to their subsystem and ensuring that the subsystem is ready for flight. The Team also has an executive board who takes care of most external relations and administrative tasks.

The Team implemented Asana for most task management, and the primary method of communication is a set of internal mailing lists. Two team-wide meetings occur every week: an all-hands meeting, where subteams discuss current progress and needs from the team; and a systems meeting, where upper level system architecture and challenges are discussed. Subteams have additional meetings throughout the week to complete tasks. The schedule is managed primarily by the President and Vice President.

¹ MIT Rocket Team, President

² MIT Rocket Team, Vice President

II. System Architecture Overview

Project Raziél is an entrant in the 2017 Spaceport America Cup 10k – COTS – All Propulsion Types category. Raziél is a 12-foot solid rocket featuring custom structures, parachutes, avionics, and payload systems. Cut-away views of the project rocket are given below.



Figure 1 - CAD render of Project Raziél

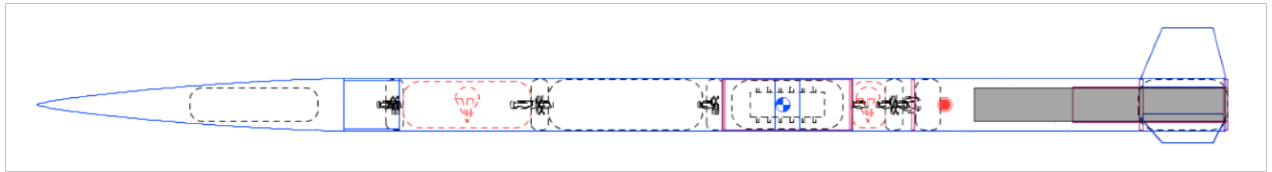


Figure 2 - Open Rocket depiction of Project Raziél

The Team sought to include as many custom designed and student built components as possible. Designs and manufacturing techniques built upon knowledge and experiences gained during previous years to increase efficiency. This rocket features an entirely custom composite airframe, including nose cone, body tubes, and fin can. The avionics utilized a student-designed flight computer, software, and ground station to initiate launch events and log flight data. Recovery utilizes a standard dual separation, dual deploy scheme with custom made ellipsoidal parachutes for both drogue and main. Lastly, the payload consists of a custom rover with an in-house designed and manufactured x-ray fluorescence sensor to determine soil composition. A detailed overview of these subsystems are given in the lettered list below.

A. Propulsion Subsystems

The propulsion system for Raziél will be a commercial Aerotech M2500-T motor.

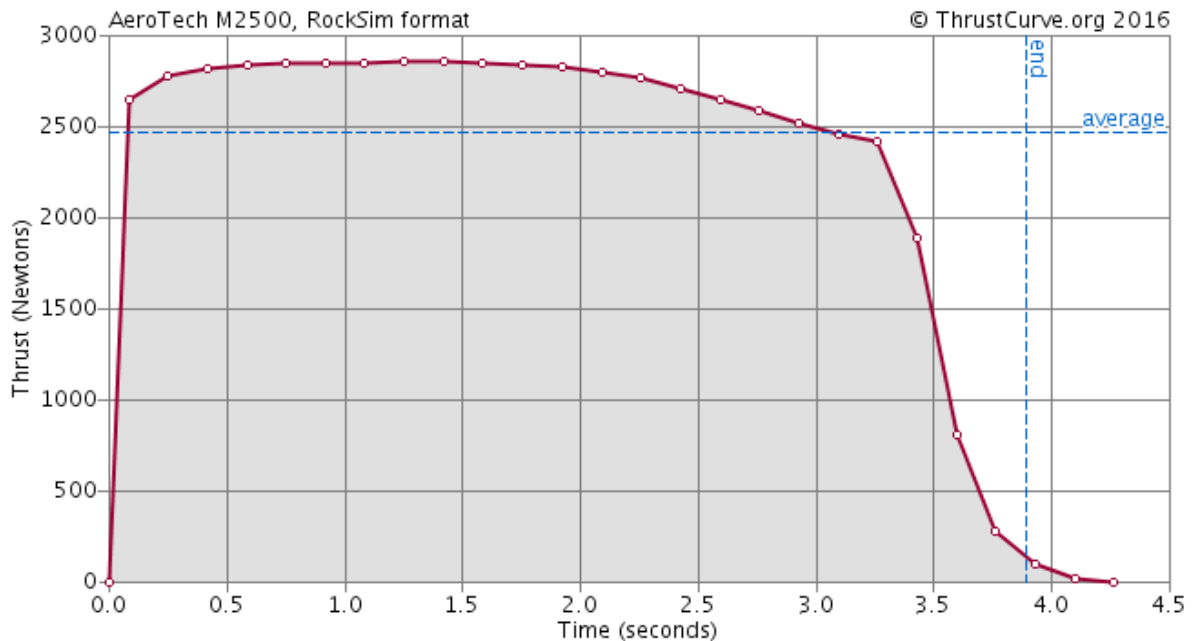


Figure 3 - Thrust curve for Aerotech M2500-T motor

This motor was selected for the following reasons:

- 1) The motor provides sufficient impulse to boost Raziel to 10000', with sufficient margin. In simulation, with 6 kg of ballast, the rocket travels to 10300'. This allows precise tuning of the amount of ballast added to the vehicle to bring the expected apogee to precisely the desired altitude to maximize performance in the competition.
- 2) The motor provides more than 8 Gs of acceleration on the launch rail. With a 15 foot rail, this will easily provide sufficient velocity off the rail ensure the vehicle is stable upon launch. Should overstability in simulation be a concern (more than 3 calibers of stability off the rail), ballast can be reorganized within the rocket to almost any configuration without compromising the stability of the rocket.
- 3) The peak thrust applied by the M2500 is very similar to the peak thrust provided during the first test flight of Raziel, which was performed using a CTI M2505-WT motor. Since the vehicle weight is approximately the same between the two tests, the acceleration and structural loading data acquired during that test will remain applicable to the competition flight.

The chosen motor is a 98mm diameter motor. This motor size was chosen after the size of the rocket was decided upon. Given the rocket size, this is the only size of the motor that can carry the vehicle to the target altitude. A 150mm motor would be at most 1 grain, which no motor manufacturer makes, and a 75mm motor would be prohibitively long. As such, a 98mm motor was chosen out of necessity, even though it creates additional drag from the wake of the rocket.

B. Aero-structures Subsystems

The airframe of Raziel achieves the purpose of safely supporting the dynamic and thrust loads of the rocket with low drag and weight. The airframe meets all of the requirements of section 6 of the ESRA Design, Test and Evaluation Guide. The team has done extensive design, testing and verification to ensure that all of these requirements are properly met. The requirements of section 6.1 are met using tested vent holes in critical areas of the rocket. The section 6.2 requirements are met with a simulated and tested composite airframe, bulkheads, fins, and aluminum fin can, as well as sturdy rail buttons to guide the rocket during take-off. Raziel is also accurately marked to fulfill the section 6.3 requirements.

1) Nose Cone Design

Since the rocket will be traveling under Mach, the Structures team chose a Von Kármán nose cone. Based on the results shown in the graphs below, the Von Karman shape has the least drag in our flight regime.

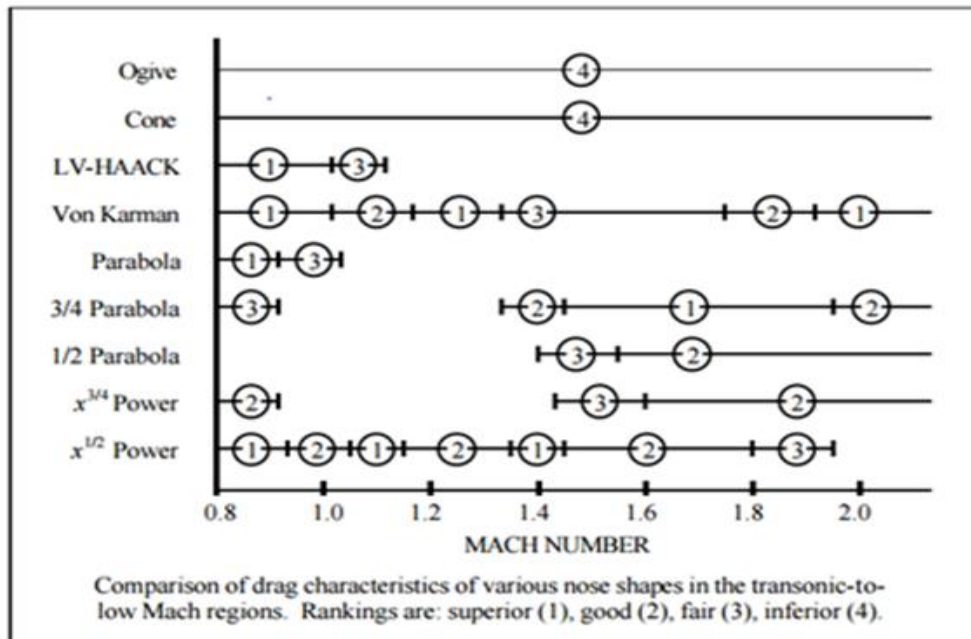


Figure 4 - Comparison of drag characteristics of various nose cones with Mach number [1]

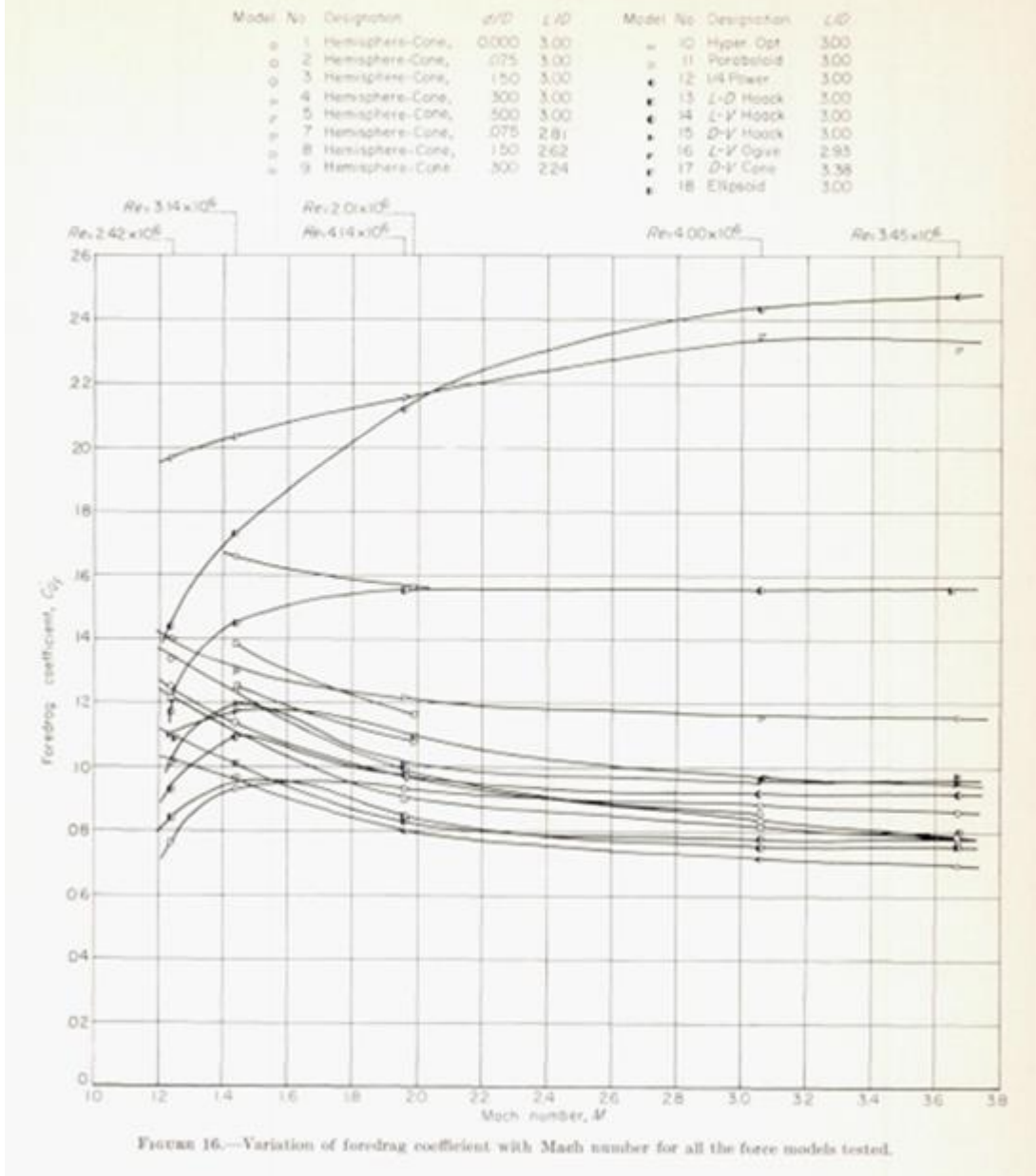


Figure 5 - Comparison of drag coefficient with Mach number [2]

Other design considerations include choosing the fineness ratio and blunting the tip. We will be using a nose cone with a fineness ratio (ratio of length to base diameter) of 5.5, since increasing the fineness ratio past 5.5 does not yield as significant a benefit as increasing fineness ratio up to 5.5, as shown in the graph below [3][4].

For lower fineness ratio nose cones, up to a fineness ratio of about 5.25, blunting the nose cone tip can decrease the drag by increasing the drag at the tip, over a small area, while decreasing the drag along the sides. Since there is not a significant difference in wave drag above a fineness ratio of 4.5, we will not make the nose cone more complicated by blunting the tip [6][7].

2) Airframe Loads

We performed an analysis of flight loads so that we could ensure that our design will fulfill requirement 6.2 on structural integrity. As you can see in the graphs below, our maximum axial load on the rocket, is 1044 N, and our maximum transverse load is 2.5 kN. Since we are using composites, we chose to design with a safety factor of

1.4, as recommended by NASA JSC 65828. This results in a 1.46 kN axial load and 3.5 kN perpendicular load. The axial stress is 30.26 KPa and the transverse stress is 486.6 Pa, both of which are well within the structural capabilities of the airframe.

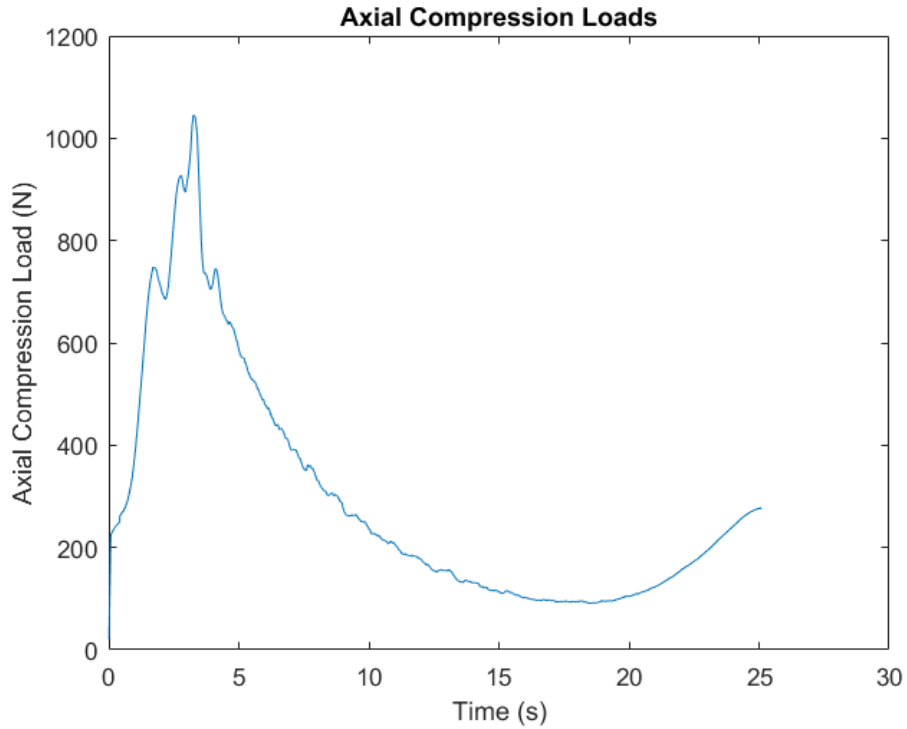


Figure 6 - Axial compression loads on rocket from launch through apogee

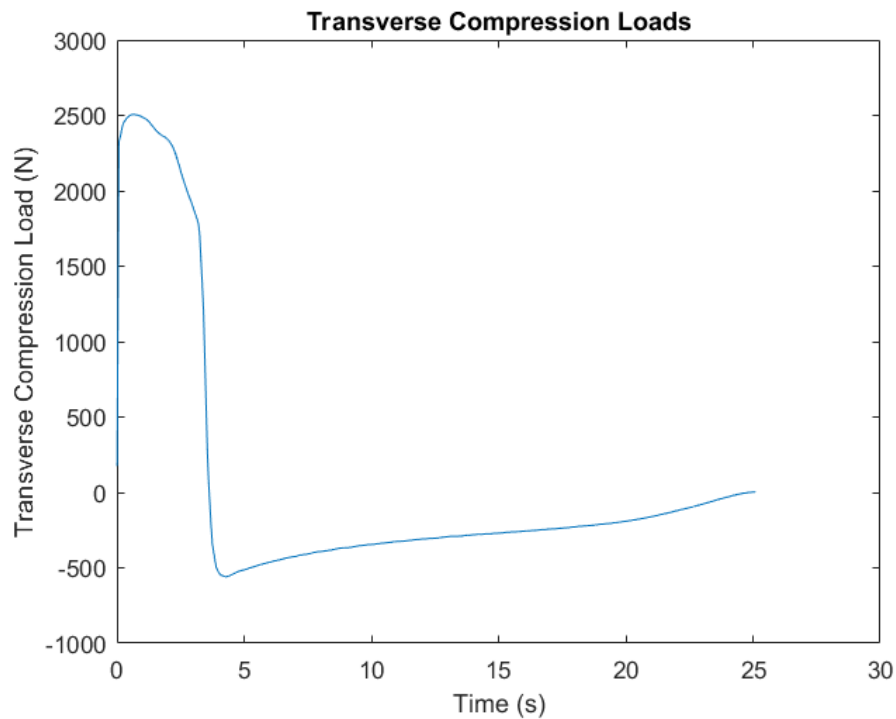


Figure 7 - Transverse compression loads on the rocket from launch through apogee

3) Airframe Testing

To fulfill requirement 6.2, the team tested composite coupons to ensure that the layup technique produced materials that could withstand the loads on the rocket. The team tested various samples, about 1" wide by 12" long, with an Instron machine to determine the modulus of the material in the longitudinal direction. The team calculated a modulus of 16 GPa, which is the modulus of the epoxy. The team used this modulus in future calculations to be conservative, but will investigate their testing procedures in the future to get a more accurate modulus. With this modulus, the team expects the tubes to deflect 0.1 mm at the maximum loading condition.

Next, the team placed the tube samples horizontally and tested them in compression. The team tested the 8" samples to 300 N, roughly double the expected transverse load on an 8" section of the rocket. The samples did not deflect. In a more fun test, one team member jumped on the 8" sample tube and did not permanently deform it. Research shows that a 160-lb person jumping exerts about 2000 N of force. Since the tubes are expected to have a transverse limit load of 2505.6 N, this test proves that the tubes have at least a 12.5 limit margin of safety.

Using this data, the team calculated that the buckling load per NASA SP-8007. The expected axial load is 1045 N, compared to a maximum axial load of 100 kN. The expected transverse load - defined differently from the calculations above - is 63 N, compared to a maximum transverse load of 61 kN. Since the current loads are such a small percentage of their expected buckling loads, buckling is not a concern. The team is confident that the tubes will withstand the flight loads.

4) Fin Geometry

The fins are specifically designed to be durable and to keep the rocket stable in flight. Different fin geometries were considered and simulated using OpenRocket software to ensure that the desired fin geometry would keep the rocket stable. The fins were specifically designed to reduce the risk of damage due to landing in several ways. A high sweep angle to tip chord ratio is used to angle the trailing edge of the fins away from the base of the rocket, eliminating stress-concentrating corners that overhang the rocket. The fins also use a high root chord to reduce the semi-span needed, in turn reducing the potential amount of torque a fin could experience from force during landing.

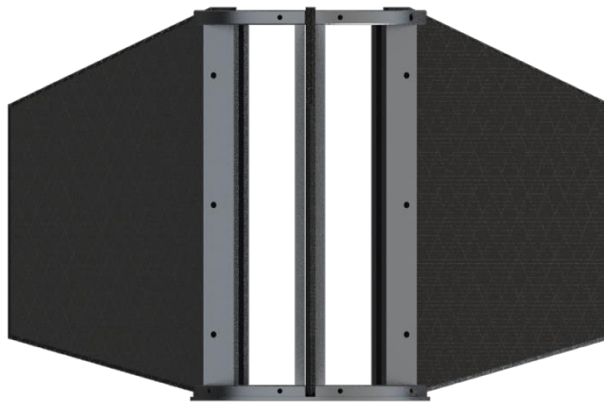


Figure 8 - Rendered image of fins integrated in the fin can in the proper alignment

5) Fin Can

Similar to last year's design, the fin can uses support struts that allow the fins to be interchangeable, in compliance with section 2.8.1.4 of the scoring guide, so that damage to the fins does not count toward damage to the vehicle. This year, the team refined the previous design for removable fins by welding the aluminum 6061 components as opposed to attaching them to the motor mount tube with epoxy. By welding the fin can, the team ensured that the aluminum structure is stronger and more permanently and accurately assembled. The team also

removed unnecessary components, like the motor mount tube and extraneous centering ring, to reduce weight and complexity. We were able to reduce the weight of the fin can from 15.5 N last year to 10.2 N this year.

These impressive weight reductions from last year were made possible by extensive structural analysis to remove unnecessary parts and lighten as many parts as possible. To analyze the structure, the team used ABAQUS to build a nonlinear model of the force interaction between the motor and the fin can structure. In particular, the model analyzes worst case loading, where the motor applies 3125N (1.25x the motor’s maximum thrust) by hard contact on the thrust ring, and the full thrust is transmitted through the fin can to the upper bolts.

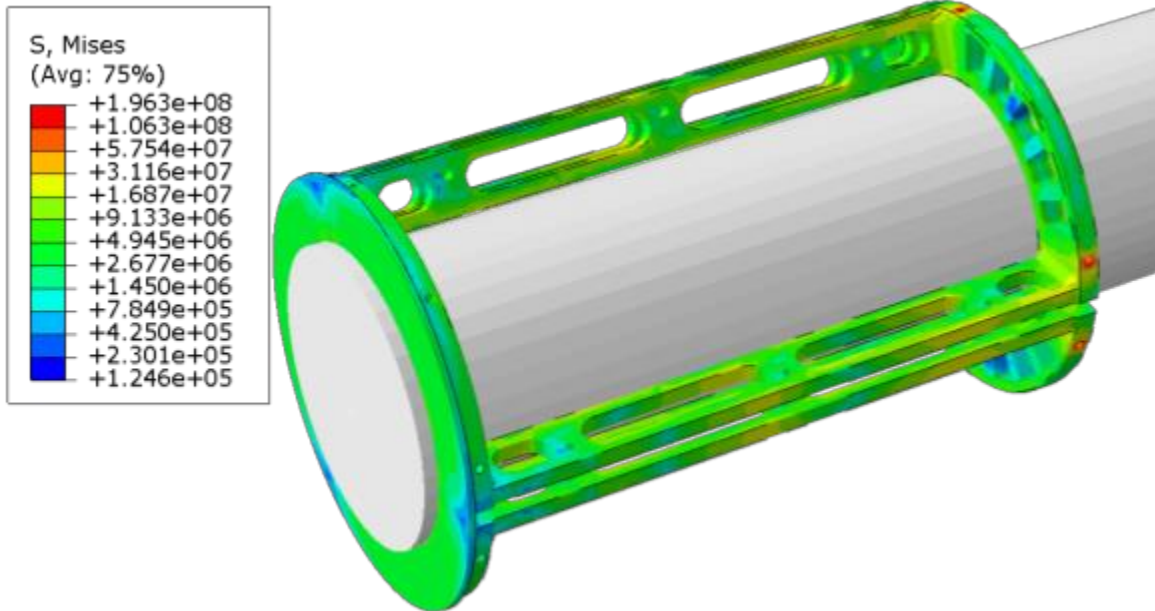


Figure 9 - FEM analysis of the fin holder at 25% safety margin on axial load

The ABAQUS analysis shows that even in this worst-case loading scenario, the entire structure is well below the alloy’s yield point, and the welded joints are an order of magnitude below the alloy’s yield point.

C. Recovery Subsystems

Raziel’s recovery system follows a dual deploy CONOPS: from apogee to approximately 1500 feet the rocket descends under a drogue parachute, while its final descent and landing is under a much larger, main parachute.

1) Streamer and Parachute Sizing and Descent Rates

Our student-made drogue parachute was proven in flight test to reduce the rocket’s speed to approximately 20 m/s. We used this data to determine an effective coefficient of drag (including the drag of the drogue and the drag of the rocket body) of 2.37:

$$\frac{1}{2} \rho V^2 A C_{D,eff,dro} = mg$$

$$\frac{1}{2} \left(1.08997 \frac{kg}{m^3} \right) \left(20 \frac{m}{s} \right)^2 \left((0.43688 \text{ m})^2 * \pi \right) C_{D,eff,dro} = (24 \text{ kg}) \left(9.81 \frac{m}{s^2} \right)$$

$$C_{D,eff,dro} = 1.80^3$$

³ Within these calculations, reference area was chosen as the largest cross section of the parachute, which is a circle with an approximately 2.87 foot diameter (0.43688 meters radius). Density was calculated using the 1976 Standard Atmospheric Model at 1200m with no temperature offset. Mass was calculated using after-burnout mass from the OpenRocket Flight Test model. It is also worth noting that the flight test also saw premature separation of the nosecone during descent under drogue. This would increase the drag acting on the rocket system—giving us a higher $C_{D,eff}$ than what we can expect for future flights.

Because we will be using the same parachute in Raziel’s competition flight, we can use this parameter to predict the drogue descent speed of the rocket in New Mexico, which corresponds to a projected after-burnout mass of 26.9 kg. We can reasonably expect, however, that our flight-day mass will vary from this computer-calculated projection (due to inaccuracies in our model, design changes, etc.). We have therefore performed these calculations using a mass sensitivity of $\pm 15\%$ (22.865 kg to 30.935kg):

$$\frac{1}{2}\rho V^2 A C_{D,eff,dro} = mg$$

$$\frac{1}{2}\left(1.08997 \frac{kg}{m^3}\right) (V)^2 ((0.43688)^2 * \pi)(1.80) = (22.865kg \rightarrow 30.935kg)(9.81 \frac{m}{s^2})$$

$$V_{dro} = 19.52 \frac{m}{s} \rightarrow 22.71 \frac{m}{s}$$

These projected descent rates lie well beneath the upper limit of the approximately 45.7 m/s range recommended by Section 3.1.1.1 of the Design Guide. Although these rates also lie slightly below the lower limit of the recommended range, we do not foresee the rocket drifting unreasonable distances.⁴ Furthermore, as was previously mentioned, we can expect the rocket to have a lower $C_{D,eff,dro}$ during the first stage of descent at the competition, leading to slightly faster descent speeds and mitigating the risk of excessive drifting.

Likewise, we used flight test data to determine the effective coefficient of drag of the rocket under its main parachute. In the flight test, we saw an approximate landing speed of 6.5 m/s, corresponding a $C_{D,eff,main}$ of :

$$\frac{1}{2}\rho V^2 A C_{D,eff,main} = mg$$

$$\frac{1}{2}\left(1.225 \frac{kg}{m^3}\right) \left(6.5 \frac{m}{s}\right)^2 (0.96 * (1.4478 m)^2 * \pi) C_{d,eff,main} = (24 kg)(9.81 \frac{m}{s^2})$$

$$C_{d,eff,main} = 1.44^5$$

Because the main parachute used during the competition will be similar in size, shape, and material, we can reasonably expect to observe a similar $C_{D,eff,main}$ during flight at the competition. Performing the same mass-range predictions described for the drogue parachute above, we yield a projected descent range of 6.34 m/s to 7.38 m/s under our 10ft diameter main parachute. This range fits comfortably within that mandated by Section 3.1.1.2 of the SAC Design Guide (under ~ 9.1 m/s):

$$\frac{1}{2}\rho V^2 A C_{D,eff,main} = mg$$

$$\frac{1}{2}\left(1.225 \frac{kg}{m^3}\right) (V)^2 (0.96 * (1.524 m)^2 * \pi) * 1.44 = (22.865kg \rightarrow 30.935kg)(9.81 \frac{m}{s^2})$$

$$V_{main} = 5.91 \frac{m}{s} \rightarrow 6.87 \frac{m}{s}$$

2) Parachute Fabrication and Strength

Both parachutes are student researched, designed, and fabricated. The parachutes are roughly semi-ellipsoidal, a shape chosen due to its high packing density. Optimal canopy loading is achieved through an aspect ratio (defined as the inflated height from the bottom of the skirt to the apex divided by the chute diameter) of 0.707. [8]

First, a student-created Matlab model was used to plot the boundary coordinates of each gore. These coordinates are then approximated to yield straight-line boundaries and used to cut out 8 parachute gores. The gores are sewn together using a “French Fell” seam, which is known for its small increase in strength over a plain seam. [9] A vent hole is cut in the drogue parachute to aid in inflation. This year’s main parachute does not contain a vent hole, increasing its drag.

Both parachutes are made from ripstop nylon fabric, which is lightweight, thin, durable, and not very permeable to air. The 0-90 ripstop reinforcement prevents tears from propagating should they arise. Much of the load on the parachute is supported by 550lb-strength paracord sewn on the seams, which detach from the canopy at the skirt and become the shroud lines.

⁴ Our experience recovering the rocket during its flight test confirms this prediction. Admittedly, apogee for the flight test was approximately 7250ft, less than the 10000ft anticipated for the competition.

⁵ Within these calculations, reference area was chosen as the largest cross section of the parachute, which is approximated as having a 10 foot diameter (1.524 meters radius). We reduced this area by 4% to account for the approximate area lost to the spill hole. Mass was calculated using the after-burnout mass taken from the OpenRocket flight test model.

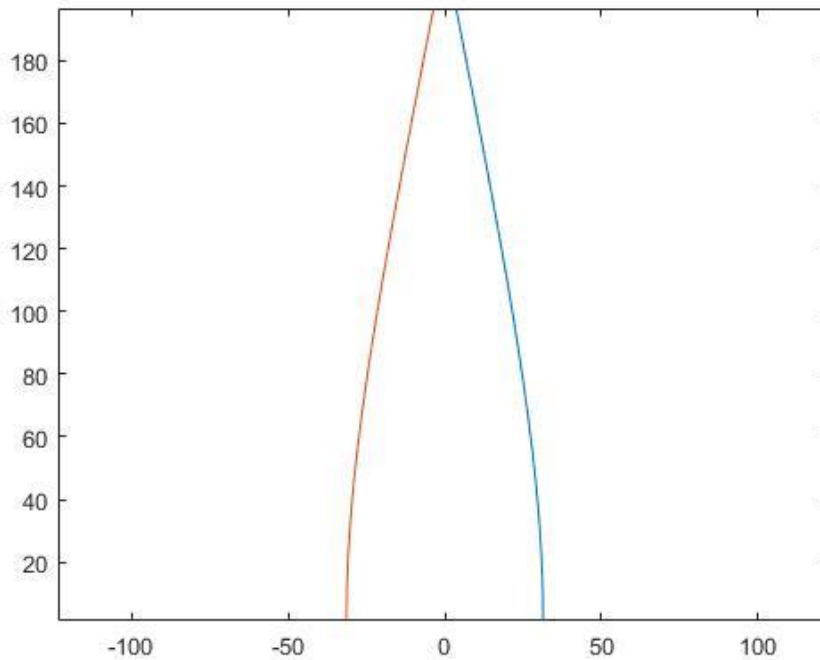


Figure 10 - Matlab model output for a 10ft diameter semi-ellipsoidal parachute gore

Lastly, per Section 3.1.3 of the SAC Design Guide, our pink and yellow drogue and red, white, blue, and black main parachutes are “colored dramatically different from one another.”

3) Black Powder Charge and Shear Pin Sizing

Three and eight-gram black powder charges eject the drogue and main parachutes, respectively. These amounts have been experimentally validated by ground testing the rocket.

The success of these charge sizes can also be predicted mathematically. The drogue is held in between the motor and the Avionics Bay, in a section of tube that is approximately 0.8 meters long. This chamber must be pressurized to approximately 7009 Pa (511.4 N) in order to break the three 4-40 shear pins attaching it to the Avionics Bay (according to a table of component strength) [10]. Using an online black powder calculator, we calculate a projected 46195 Pa from our 3g charge size, yielding an approximate 6.6 times safety factor in our design [11].

The main parachute is held above the Avionics bay, in a long section of tube that extends into the nosecone. For the purposes of calculating safety factor, we neglect the volume consumed by the parachute and payload and model the nosecone space as another body tube.⁶ Using the same black powder calculator with a charge size of 8 grams, we yield a projected 75842 Pa. The projected force to break four size 6 shear pins (using data taken from the aforementioned component strength table) is 1075.8 Newtons (67699 Pa), which indicates a roughly 1.12 times safety factor.

4) Data Collection Rig

Although there are several models of parachute deployment, they all are either too computationally expensive or too approximating to predict stress for a linked-body, canopy-first recovery system. The dynamics of a parachute, a free permeable tension structure, moving through a compressible fluid are complex and chaotic enough that even coupled fluid-structure interaction codes for simple, controlled systems yield highly uncertain projections [5]. Thus, experiment is the only method to verify decelerator design. Furthermore, full flight tests are, within the resources of the team, the only method of testing high-speed, finite-mass deployment.

⁶ This means that our system is even safer than our margin reflects.

Three cameras and two inertial measurement units collect flight data, which is used to calculate inflation time and characteristics, parachute drag area, parasitic oscillation, and total force on the avionics body section. To measure the force on the body by the parachute, the recovery team developed a strain gauge which connects in series with the main riser. The milled aluminum dogbone has a resistive strain gauge mounted in a quarter-bridge arrangement. After amplification, Pyxida acquires the data. This particular measurement is critical to determining if increasing shear-pin strength safely mitigated premature nosecone separation caused by drogue deployment, which was observed during the flight test. The gauge will characterize snatch (line-stretch) force, commonly an issue during canopy-first deployment, and inflation-shock force. Together, the data will help identify possible failure modes, be key in determining drag from the parachute alone, help determine which recovery components should be strengthened and which lightened, focus research and development efforts into methods to reduce development loads, and inform future decelerator system design.

5) Trajectory and Landing Analysis

In order to ensure that the rocket will not drift onto the White Sands Missile Range (WSMR), an analysis of historical wind data and corresponding rocket trajectories was conducted. Average wind speeds and headings for the Truth or Consequences Municipal Airport for June 22-24 for the past 50 years were gathered as a basis for predicting the expected wind speed and heading for this year. With this wind data, a 95% confidence ellipse was calculated and drawn to determine the region that, with 95% confidence, will include the average wind speed and heading for this year. Since the worst-case largest eastern wind component will yield the worst case landing location in the eastern direction, it is sufficient to simulate the rocket trajectory with these conditions to ensure the rocket will not land on the WSMR. The largest eastern wind component existing inside the confidence ellipse was calculated and determined to be 4.15 m/s at a heading of 59.14°. A plot of the wind data, confidence ellipse, and point of largest eastern wind can be seen in the figure below.

95% Confidence Ellipse for Wind Heading (degrees) vs. Speed (m/s)

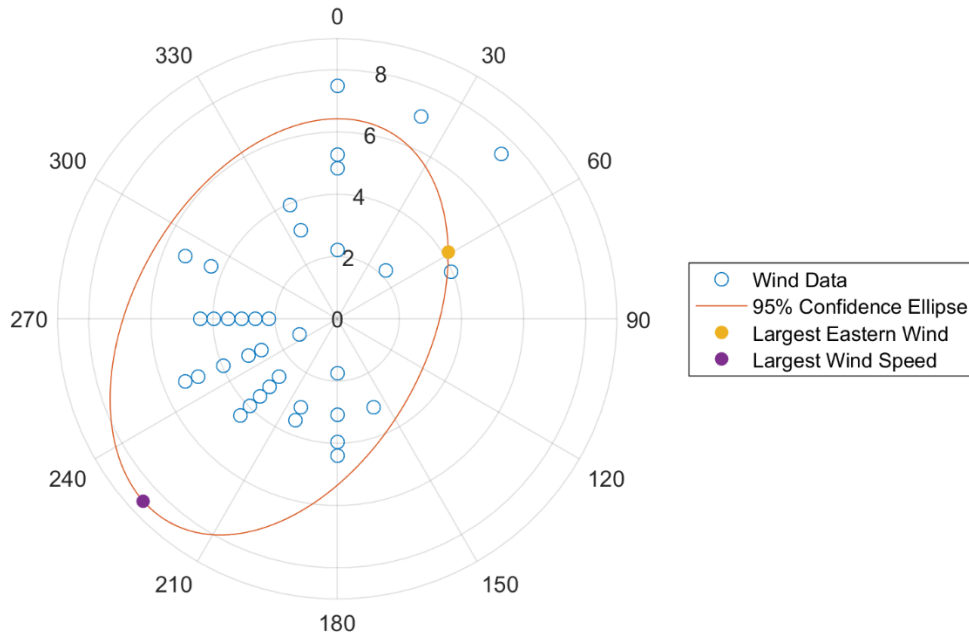


Figure 11 - Wind data and confidence ellipse for Truth or Consequences, NM

After the point of largest eastern wind was determined, the values were used to simulate the rocket trajectory in Open Rocket. The corresponding landing location was determined to be 148 meters north and 240 meters east of the launch site. From this, it can be concluded that in worst case conditions, the rocket will not drift onto the WSMR.

We then analyzed the maximum ground distance recovery forces may need to traverse to recover the rocket. The 95% bound wind conditions yield a maximum wind velocity of 8.7 m/s on a heading of 226.75°. Simulating this yields

a vehicle displacement at a landing of 685 meters south and 733 meters west of the vertical launch facility, for a total over ground distance of 1,003 meters from the launch site. This is within walkable recovery distance with appropriate environmental preparation.

D. Avionics Subsystems

The rocket is equipped with a redundant pair of flight computers that are responsible for recovery and tracking. The first is an Altus Metrum Telemetrum, which is a COTS system that the team has significant experience with. The second is a system called Pyxida that the team developed. The hardware component of Pyxida is a microcontroller, radio, and set of sensors that inhabit a custom PCB.

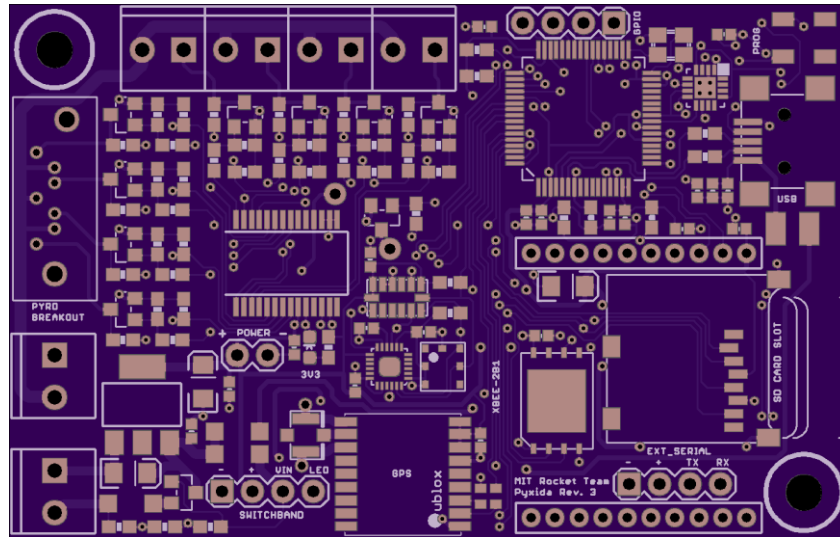


Figure 12 - Pyxida custom PCB design

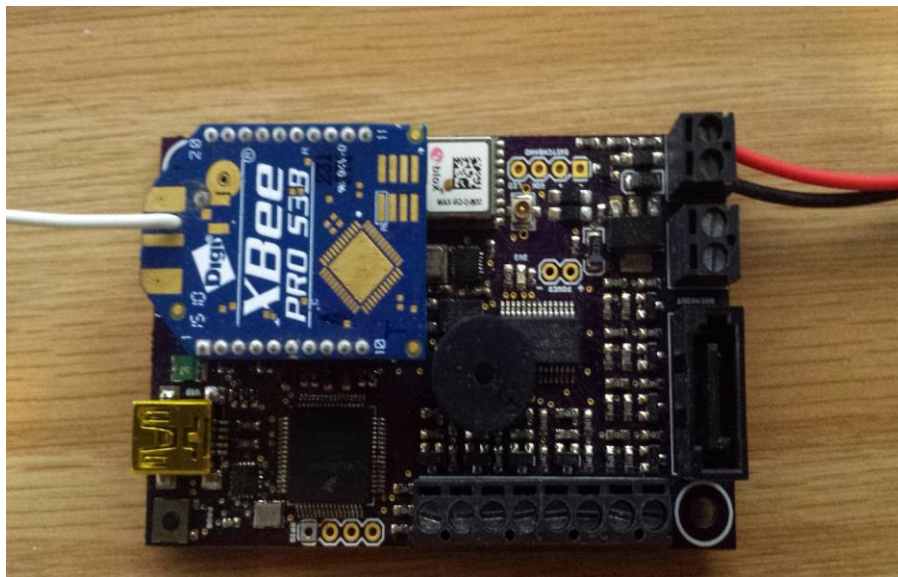


Figure 13 - Image of Pyxida PCB with all components installed

The Pyxida system includes two software packages. The first is the firmware that runs on the flight computer hardware itself, which is written in C++. It is responsible for gathering data from sensors, filtering it, and using it to track the state of the rocket. The firmware is based on a state machine that includes states for each phase of flight. State changes are determined by the output from the state estimator, which uses data from multiple sensors to

determine the rocket's position and attitude. When state changes occur, pyrotechnic events can be triggered based on the configuration stored in the device's flash memory. In addition to the state machine, the firmware also logs sensor data to the on board memory and sends it over the radio to the ground station. This overall design was selected because the required behaviours during the different phases of the mission are too diverse to run the same procedures throughout the entire flight.

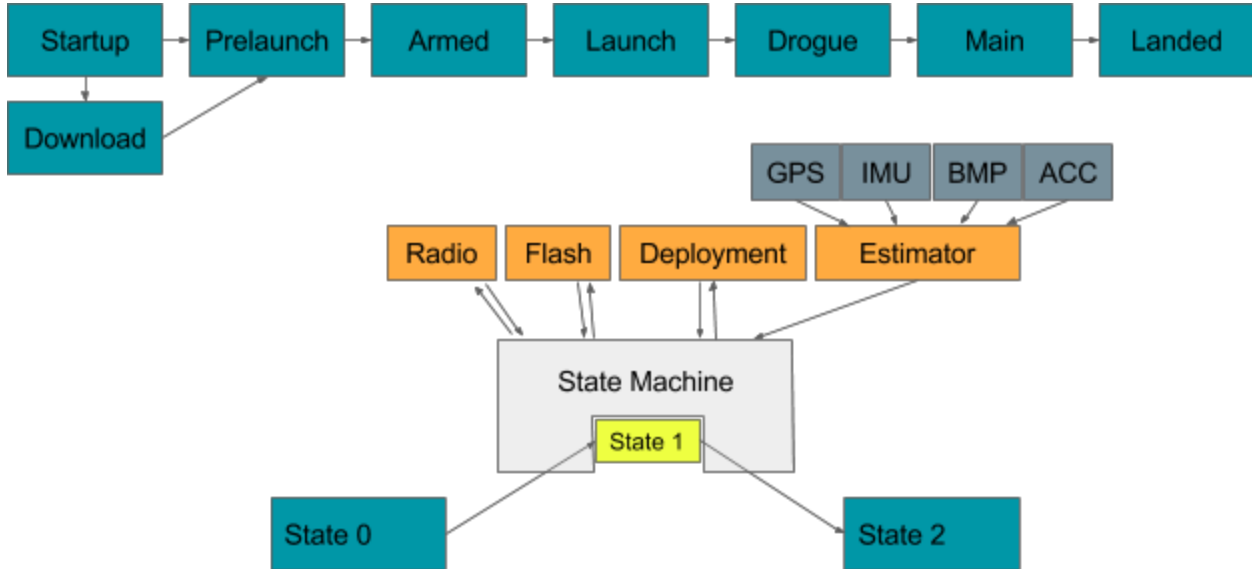


Figure 14 - Phase management and data flow architecture for Pyxida software

The second piece of software in the system is the ground station, which is a GUI application that allows a user to set up flight configurations, monitor sensor data during flight, and graph data after the rocket has been recovered.

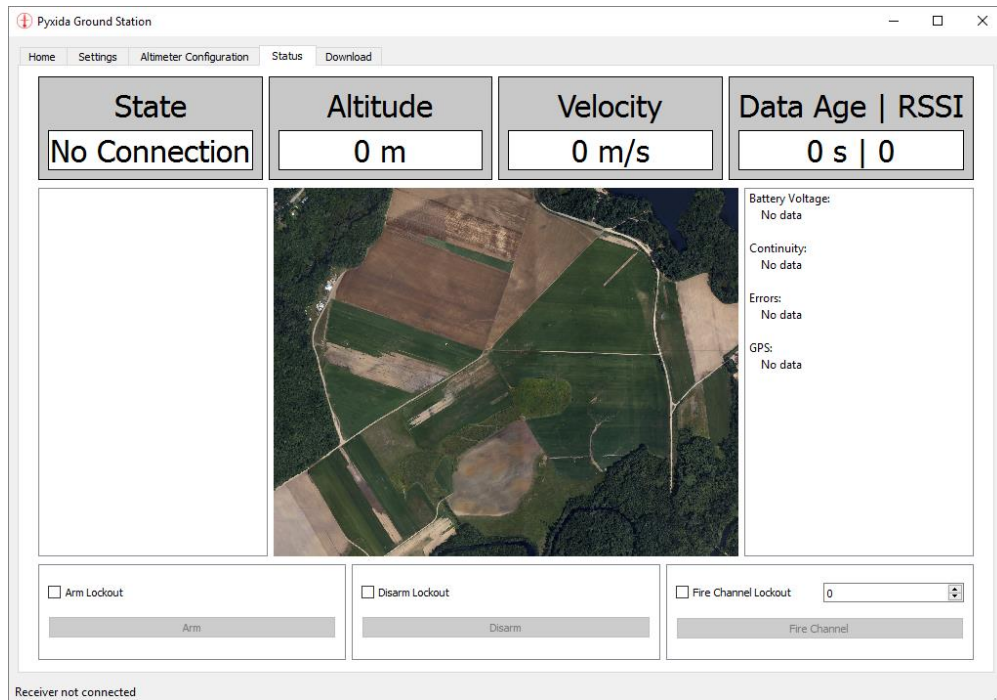


Figure 15 - Image of Pyxida Ground Station GUI

Power is provided to all avionics systems through a small power distribution board mounted in the center of the avionics sled. Battery power is routed to this board through Dean's connectors that are soldered on, and leaves the board via JST connectors. Both of these connectors allow for power to be quickly removed from the system without cutting wires. The switches for enabling and disabling the flight computers are also routed to this board, where they are used to interrupt the flow of power from the battery to the flight computer until the rocket is vertical.

E. Payload Subsystems

The payload consists of three main structures: the enclosure, the rover, and the sensor. It also has a deployment mechanism, the sabot.

The enclosure is a cuboidal aluminum frame used to protect the rover during ascent and landing. It measures 1Ux1Ux3U, or 10cmx10cmx10cm, to comply with the cubesat size requirement. It attaches to the sabot, two pieces of fiberglass-reinforced foam that conform to the inner diameter of the tube and allow the enclosure to smoothly exit the rocket. After after detecting landing, the enclosure/sabot structure opens, allowing the rover to exit. The sabot/enclosure structure is spring-loaded to open, but is held closed during ascent and landing using paracord. Once landing is detected by the avionics, a charge is sent to a pyrotechnic rope cutter, which severs the paracord, allowing the enclosure/sabot structure to spring open and the rover to deploy.

Once the sabot opens, the rover exits. The rover has three main components: the chassis, the wheels, and the flight computer. The chassis is a hexagonal prism made of sheet aluminum. The wheels are 3D printed, and use springs to passively expand as the rover exits the sabot. This allows for a greater ground clearance without decreasing the size of the chassis itself. Finally, the rover is controlled by a Teensy microcontroller. The microcontroller executes an autonomous driving mission using a pre-programmed straight-line trajectory, and uses open loop control.

The sensor determines soil density and composition using the x-ray fluorescence techniques. The sensor will use a source of ionizing radiation to excite x-ray fluorescence in high-Z materials in the soil beneath the rover (both a beta source and a x-ray source are in development). These photons will then be detected by a PIN diode attached to the bottom of the rover. The sensor (SFH0206K) has been chosen such that the system will be able to detect k-alpha lines from elements with $Z > 26-29$. The differential attenuation of the various detected k-alpha lines can then be used to determine the approximate soil density. Depending on future test results, the sensor may be cooled by a thermoelectric cooler (TEC) to reduce thermal noise and prevent gain drift.

The other major component of the system is a Fe-55 beta source from Spectrum techniques behind a graded-Z shutter which can be remotely controlled. The source is aligned within the collimator such that a beam of beta particles ~ 10 mm diameter impacts the soil approximately normal to the surface below the rover. The scintillation detector is offset from the source axis and aligned such that the axis of the scintillator points towards the area where the beta particle beam impacts the soil (to detect and XRF photons). A secondary system employing an ultra-compact x-ray tube is also under development, and may offer a cleaner XRF signal (as there are no scattered betas to be concerned with).

The system currently has noise issues due to a switching DC/DC converter that radiates a large amount of HF noise. Current work is focused on reducing this using mu-metal shielding.

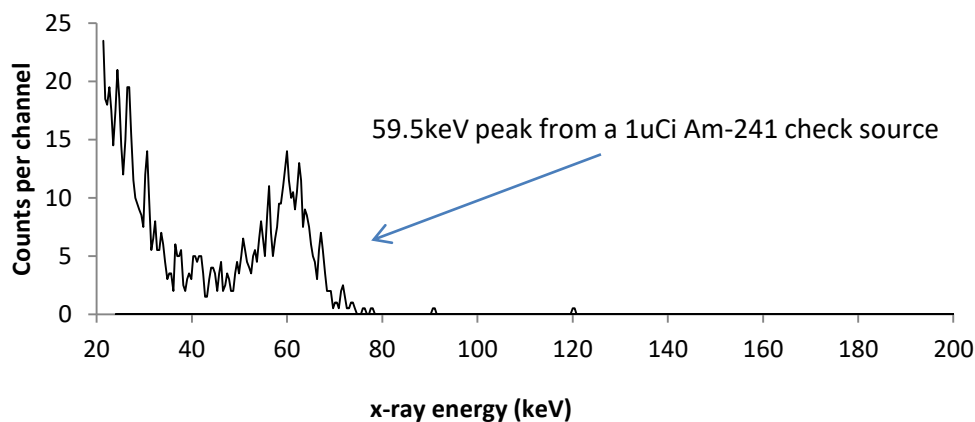


Figure 16 - This x-ray energy spectrum was the result of 10min of data gathered with the SFH0206k photodiode using a 8us shaping amplifier (CREMAT CR-200) and a CR-110 charge sensitive amplifier. The pulses were stretched to $\sim 100\mu$ s and then digitized using a phone

When the rocket is integrated, the payload is located at the aft end of the payload and recovery tube, below the main parachute. It has one u-bolt, which is connected to an eyebot at the end of the avionics bay and the main parachute using webbing and quicklinks. The payload is deployed with the main parachute; the main parachute charge pressurizes the entire payload and recovery tube, pushing out both the main and the payload. The payload lands with the rest of the rocket, then opens as described above.

III. Mission Concept of Operations

Project Raziel utilizes an Aerotech M2500-T motor to boost it to its apogee of 10,000 feet. A standard dual separation, dual deploy recovery scheme is utilized to recover the rocket, with drogue deploying at apogee and main deploying at 1,500 feet. At main deployment, the payload enclosure is deployed, which lands at the same time as the rest of the rocket. After the landing, the rover is deployed from it's enclosure, and the sensor begins collecting data on the soil composition. An illustration of this sequence of events is depicted below.

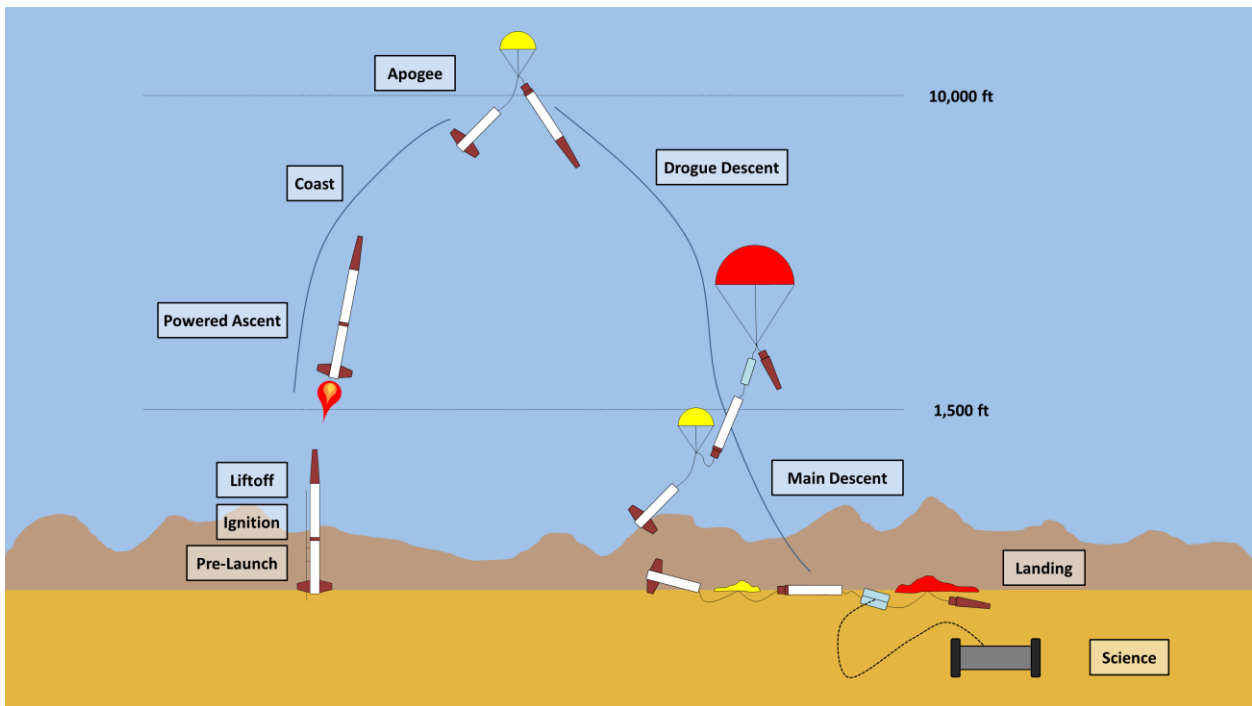


Figure 17 - Concept of Operations for Project Raziel flight

Additionally, the flight can be divided into a series of phases with specific entrance and exit criteria. These phases, entrance and exit criteria, as well as corresponding verbal descriptions are given in the table below.

Table 1 - Concept of Operations Phase Table

Phase	Entrance Criteria	Description	Exit Criteria
Prelaunch	Launch rail approach	Team members bring Raziel to the launch pad. The rocket is slid onto the launch rail. Avionics are armed, and the motor is connected to the ignition system. The Team members then exit the launch area to the flight line.	Countdown
Ignition	Countdown	The motor is ignited by the ignition system and comes up to pressure.	Motor pressurization
Liftoff	Motor pressurization	The rocket begins ascent, and exits the launch rail.	Launch rail exit
Powered Ascent	Launch rail exit	The rocket motor continues to burn, and the rocket accelerates towards apogee.	Motor burnout

Coast	Motor burnout	The rocket motor is no longer burning, and the rocket continues on an upward trajectory.	Rocket reaches maximum altitude
Apogee	Rocket reaches maximum altitude	The rocket reaches its maximum altitude and deploys the drogue parachute.	Drogue chute exits its section.
Drogue Descent	Drogue chute exits its section.	The rocket descends under drogue from apogee to 1500 feet AGL, at which point the main is deployed.	Main chute inflation
Main Descent	Main chute inflation	The rocket safely descends under the main parachute after its inflation.	Rocket ground impact
Landing	Rocket ground impact	The rocket lands. The payload begins its science mission by deploying the rover from the sabot.	Rover deployment from sabot
Science	Rover deployment from sabot	The rover orients itself, and its sensor collects data about the surrounding soil. The rover completes a short drive mission.	Rover completes sensing and drive missions

IV. Conclusions and Lessons Learned

The process of designing and building Raziel has proved to be very challenging. However, through these challenges, the Team has benefitted greatly through the many lessons learned.

One of the key lessons that the Team learned is the importance of integration and communication. Throughout the year, subteams made designs and manufactured parts for the rocket. However, even though all would seem well in the technical drawings, upon integrating the rocket and evaluating the interface between two subteams, it often became apparent that two parts were incompatible. The Team found that miscommunications and poor documentation often led to hardware not integrating correctly, and cost the team both time and money to remedy these mistakes and manufacture new parts. However, from these mistakes, the Team has greatly improved their communication and documentation. A master CAD model for all subteams is now managed to ensure that parts made by any subteam is compatible with other hardware. Furthermore, a weekly team-wide systems meeting helps to ensure that everyone is aware of what other subteams are doing, reducing many miscommunications.

The Team actively works to make sure all lessons learned and technologies developed are documented and knowledge is transferred efficiently from upperclassmen to underclassmen. In the last year, the Team has implemented an online Wiki, where team members document their projects and insights so that it will always be available to future members on Rocket Team. Team documents are also stored on an online server so that documents are not lost when team members graduate. Additionally, exec members and subteam leads are chosen several months in advance of the actual start of their new position, so that the current Exec and subteam leads may have time to transfer their knowledge to these new people. These efforts have proved to be very successful in transferring and maintaining the knowledge of the team, even though actual team membership changes every year.

Appendix

The following appendices provide additional information for Project Raziel.

A. System Weights, Measures, and Performance Data

Below is the third and final Progress Report, which satisfies the requirement for this appendix.



Color Key	SRAD = Student Researched and Designed	v17.1
Must be completed accurately at all time. These fields mostly pertain to team identifying information and the highest-level technical information.		
Should always be completed "to the team's best knowledge" , but is expected to vary with increasing accuracy / fidelity throughout the project.		
May not be known until later in the project but should be completed ASAP, and must be completed accurately in the final progress report.		

Submit Date: 5/29/2017

Team ID: 35

* You will receive your Team ID when you submit your project entry form.

Team Information

Rocket/Project Name:	Project Raziel	
Student Organization Name	MIT Rocket Team	
College or University Name:	Massachusetts Institute of Technology	
Preferred Informal Name:	MIT	
Organization Type:	Club/Group	
Project Start Date	8/1/2016	<small>*Projects are not limited on how many years they take*</small>
Category:	10k – COTS – All Propulsion Types	

Member	Name	Email	Phone
Student Lead	Andrew Adams	adamsa@mit.edu	919-886-9406
Alternate Contact	Andrew Kurtz	akurtz@mit.edu	857-209-4875
Faculty Advisor	Warren Hoburg	whoburg@mit.edu	617-253-1207
Alternate Faculty	Paulo Lozano	lozano@mit.edu	617-258-0742

For Mailing Awards:

Payable To:	MIT Rocket Team
Address Line 1:	Attn: Sandra Lipnoski
Address Line 2:	Massachusetts Institute of Technology
Address Line 3:	77 Massachusetts Avenue
Address Line 4:	Building 4-408
Address Line 5:	Cambridge, MA 02139

Rocket Information

Overall rocket parameters:

	Measurement	Additional Comments (Optional)
Length (inches):	141	
Max Diameter (inches):	6.2	
Vehicle weight (pounds):	50.1	* Payload not included in vehicle weight - also w/o propellant here
Liftoff weight (pounds):	69.6	
Number of stages:	1	* Not including Kinetic Energy Dart
Strap-on Booster Cluster:	No	
Propulsion Type:	Solid	
Propulsion Manufacturer:	Commercial	AeroTech
Kinetic Energy Dart:	No	

Propulsion Systems: (Stage: Manufacturer, Motor, Letter Class, Total Impulse)

1st Stage: AeroTech, M2500T, M Class, 9600 Ns

Total Impulse of all Motors: 9600 (Ns)

Predicted Flight Data and Analysis

The following stats should be calculated using rocket trajectory software or by hand.

Pro Tip: Reference the Barrowman Equations, know what they are, and know how to use them.

	Measurement	Additional Comments (Optional)
Launch Rail:	Other	Doug Gerrard's Rail
Rail Length (feet):	18	Changed since 2nd report
Liftoff Thrust-Weight Ratio:	7.6	Changed since 2nd report
Launch Rail Departure Velocity (feet/second):	93	Changed since 2nd report
Minimum Static Margin During Boost:	1.8 calibers	Changed since 2nd report
Maximum Acceleration (G):	8.7	Changed since 2nd report
Maximum Velocity (feet/second):	900	
Target Apogee (feet AGL):	10000	
Predicted Apogee Altitude (feet AGL):	9970	

Payload Information

Payload Description:

The payload is a rover-based science mission performing soil analysis using x-ray fluorescence techniques. In addition, a reach goal of the rover is to perform a basic drive mission. To determine soil density and composition using the XRF technique, the rover will use a source of ionizing radiation to excite x-ray fluorescence in high-Z materials in the soil beneath the rover (both a beta source and a x-ray source are in development). These photons will then be detected by a PIN diode attached to the bottom of the rover. The sensor (SFH0206K) has been chosen such that the system will be able to detect k-alpha lines from elements with $Z > 26-29$. The differential attenuation of the various detected k-alpha lines can then be used to determine the approximate soil density. Depending on future test results, the sensor may be cooled by a thermoelectric cooler (TEC) to reduce thermal noise and prevent gain drift. The other major component of the system is a ^{55}Fe beta source (3.7MBq) from Spectrum techniques behind a graded-Z shutter which can be remotely controlled. The source is aligned within the collimator such that a beam of beta particles $\sim 10\text{mm}$ diameter impacts the soil approximately normal to the surface below the rover. The scintillation detector is offset from the source axis and aligned such that the axis of the scintillator points towards the area where the beta particle beam impacts the soil (to detect and XRF photons). A secondary system employing an ultra-compact x-ray tube is also under development, and may offer a cleaner XRF signal (as there are no scattered betas to be concerned with).

Recovery Information

Payload Recovery Method:	Parachute	
--------------------------	-----------	--

1st Stage Recovery:

Additional Comments

Type:	Parachute	
Primary Initiation Sensor:	Barometer	
Secondary Initiation Sensor:	Barometer	
Deployment energy Source:	Black Powder	

2nd Stage Recovery: (If Applicable)

Additional Comments

Type:	Parachute	This is the 2nd deployment for the 1st stage
Primary Initiation Sensor:	Barometer	
Secondary Initiation Sensor:	Barometer	
Deployment energy Source:	Black Powder	

3rd Stage Recovery: (If Applicable)

Additional Comments

Type:		
Primary Initiation Sensor:		
Secondary Initiation Sensor:		
Deployment energy Source:		

Strap-On Booster Recovery: (If Applicable)

Additional Comments

Type:		
Primary Initiation Sensor:		
Secondary Initiation Sensor:		
Deployment energy Source:		

Kinetic Energy Dart: (If Applicable)

Additional Comments

Type:		
Primary Initiation Sensor:		

Secondary Initiation Sensor:		
Deployment energy Source:		

Planned Tests

* Please keep brief

Date	Type	Description	Status	Comments
9/15/1 6	Ground	Strand Burns (first round)	Minor Issues	Some burns completed, equipment malfunction
11/1/1 6	Ground	Small scale propulsion test - 54mm motors	Successful	Validated mixing process, thrust model, test equipment
1/19/1 7	Ground	Recovery Ground Test - CO2, BP	Minor Issues	Switched to all BP.
2/28/1 7	Ground	Structural Coupon testing	Successful	Validate FEA, epoxy system
3/5/17	Ground	Rover Testing	Successful	Test Rover Drive sequence
3/11/1 7	Ground	Static Fire - 98mm, 1 grain	Successful	Validate mixing & thrust model for 98 mm
4/2/17	Ground	Static Fire - Flight Motor	Major Issues	Descoped to COTS Propulsion
4/5/17	Ground	Avionics Vacuum Test	Successful	Validate deployments, flight prep
4/5/17	Ground	Recovery Ground Testing	Successful	Most recent rocket changes validated
4/9/17	In-Flight	Flight Test 1	Minor Issues	Successful flight, some changes needed
4/20/1 7	Ground	XRF Sensor Testing	Successful	Good initial science data, ready for rocket
5/1/17	Ground	Rover Deployment Testing	Successful	Rover/sabot deployment evaluated
5/11/1 7	Ground	Recovery Ground Test	Successful	Shear pin changes validated

Any other pertinent information:

Some of the above tests occur over several weeks (e.g., strand burning), and only one date is given for conciseness. Many of the tests that were performed are not listed above. Raziel was ground tested a total of 8 times for recovery in different configurations throughout the program, and the avionics suite is periodically vacuum tested as the hardware was iterated. Key dates/decisions are included in the above table, including the work for the custom propulsion, which was cancelled in mid-April in favor of a COTS system.

B. Project Test Reports

Recovery System Testing:

The Recovery system's primary form of testing comes in the form of ground tests. Ground tests were conducted throughout the year, reflecting periodic changes in design and/or charge size. Within these hobby-standard tests (conducted on MIT's Brigg's Athletic Field), charges are ignited from within the rocket, separating sections from which parachutes will emerge in flight. These tests are primarily used to verify charge size, although they can also be used to identify integration challenges and design flaws.

The most recent ground test (and most representative of Raziel in its competition configuration) was conducted on May 17th, 2017. Within this test, 3 and 8 gram charges were used to separate the fin can from the Avionics Bay and the payload tube from the nosecone, respectively. Wires running from these charges to a voltage source far from the rocket were used for ignition.

As is visible in the video still below, 3g of black powder was highly successful in separating the fin can from the Avionics Bay. The force of the ejection event itself was enough to begin to unravel and draw out the Recovery related equipment (i.e. large amounts of webbing, the drogue, and Nomex, all of which are featured in the second photo below).



Figure 18 - Image of the rocket following separation of the fin can by a 3g black powder charge



Figure 19 - Image of the drogue being drawn out of the rocket tube - a sign of a successful ejection event

Likewise, the 8g main charge event was also extremely successful. This amount of black powder yielded a highly energetic event, fully drawing out our simulated payload as well as our main parachute's deployment bag (which is resting by the nosecone). We did not anticipate that the payload tube and nosecone would travel as far as they did. We hypothesize that the strength of the four size 6 shear pins enabled the combustion gas to build up prior to shearing, increasing the kinetic energy of the moving bodies upon release. It is worth noting that we manually disconnected the Avionics Bay from the fin can between the drogue and main tests (as is visible below), although this modification would not yield any significant difference in testing results (had the two been connected the weight of the fin can might have reduced the distance traveled by the payload tube).



Figure 20 - Image of the rocket following the main 8g charge separation event

The rocket will admittedly undergo some changes between this ground test and the competition. Most notably, the ballast used in flight will likely be different from the ballast used in test. Likewise, our actual payload will be installed, instead of just a mass simulator (which are the purple pieces between the nosecone and the payload tube in the photo above). These changes do *not* invalidate the results of the May 17th ground test, nor do they decrease our confidence in the system. As is evident in the video stills above, our tested charge sizes are more than able to withstand these kinds of variation in the system.

Raziel's recovery system is controlled by two altimeters, our student-designed flight computer, Pyxida, and a commercial Telemetry. Both are capable of handling all recovery events and are completely independent from one another. Each has its own battery and is hooked up to separate black powder charges by separate e-matches. Furthermore, each of these charges is sufficient to yield a successful ejection event by itself. Thus, one system can completely fail without compromising the ability of the other system to command a successful recovery sequence. Prior to flight, we can choose our desired firing delays between the two systems. Although we may revise our plan, we currently anticipate that the COTS Telemetry will fire the drogue charge one second before Pyxida fires its drogue charge. Similarly, the Telemetry will be first to fire its main parachute charge, with Pyxida following a few hundred feet below.

This information is summarized in the schematic below:

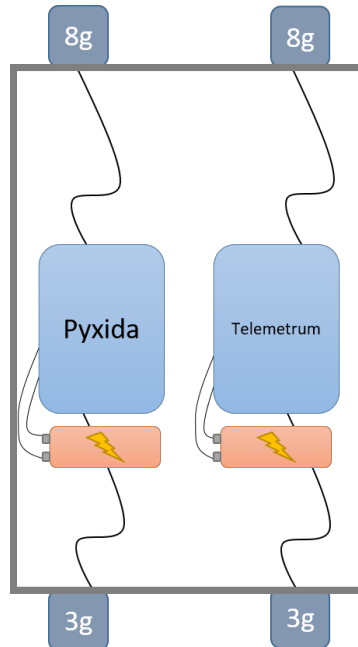


Figure 21 - Schematic illustrating the redundancy of Raziel's recovery electronics

SRAD Propulsion System Testing

THIS PAGE INTENTIONALLY LEFT BLANK

SRAD Pressure Vessel Testing

THIS PAGE INTENTIONALLY LEFT BLANK

C. Hazard Analysis

The MIT Rocket Team will follow appropriate safety procedures as specified by the Experimental Sounding Rocket Association and the National Association of Rocketry High Power Safety Code in order to mitigate hazards associated with the operation of Raziél.

The largest hazard associated with Raziél is interacting with the motor. To mitigate this hazard, the motor will not be installed into the rocket until all other systems are integrated and the rocket is ready to be walked to the launch pad. The motor will be transported with the upmost caution and wrapped in soft material to prevent damage to the motor. The igniter will not be installed into the motor until the rocket is vertical on the launch pad and only critical personnel remain at the launch pad. Any personnel at the launch pad will wear safety glasses until they are at least the minimum safe distance away from the rocket. All other personnel will be at least the minimum safe distance away from the rocket. The altimeters (hence the black powder ejection charges) will be armed remotely from a SRAD ground station once all personnel are at least the minimum safe distance away from the rocket.

A second hazard is created by the use of an NRC-exempt Fe-55 sealed source (under one micro-curie) for our XRF sensor on the rover payload. This hazard is mitigated by the use of a lead columnator, which only opens on command from the rover computer for a brief moment during science operations. In addition, operators of the payload will be using sensitive Geiger counters throughout the assembly of the payload and rocket. In addition, the primary operator of the payload has extensive experience with sources of this type. After being cleared by Bill Gutman (NMSA) earlier this year, we ensured the safety of the team throughout the build and test of this sensor.

Other hazards arise out of keeping black powder on the launch site. To mitigate, black powder and igniters will be transported and stored in ammunition boxes until they are integrated into the rocket. Ammunition boxes and black powder containers will be clearly labelled with the contents. The team members integrating the rocket will wear the proper personal protective equipment (safety glasses or a face shield) while preparing the recovery system.

D. Risk Assessment

A risk assessment matrix summarizing failure modes that pose a risk to mission success is given below.

Table 2 - Risk Assessment Matrix

Team	Rocket/ Project Name	Date	Note: Referenced ESRA Risk Matrix for several common hazards, and format of risk matrix.		
<u>MIT Rocket Team</u>	<u>Project Raziél</u>	<u>5/29/17</u>			
Hazard	CONOPS Phase(s)	Possible Causes	Risk of Mishap and Rationale	Mitigation Approach	Risk of Injury after Mitigation
Recovery system deploys during prelaunch, causing injury	Prelaunch	Avionics prematurely armed	Low, COTS altimeter and custom altimeter do not arm immediately	Custom flight computer armed with ground station	Low
		Static electricity ignites BP charges on the ground		Copper Charge canisters provide ground	
Rocket falls from launch rail during prelaunch preparations, causing injury	Prelaunch	High winds cause rocket to shake	Low, using Doug's rail. Presented no problems in high winds with last year's project, which was more top heavy and the same diameter as Raziél.	Follow prelaunch procedures	Low

		Improper balancing of the rocket during raise		Team experience with rockets falling from launch rail.	
		Improper balancing of the launch pad during setup			
Rocket does not ignite when command is given ("hang fire"), but does ignite when team approaches to troubleshoot	Ignition	Small pieces of propellant initially burn but do not generate enough pressure right away to quickly pressurize.	Low, fast-burning propellant, COTS motor	Wait for 60 seconds before approach	Low
Catastrophic failure of rocket motor	Ignition, Liftoff, Powered ascent	Chunks of propellant break off during the burn	Low, COTS Motor	Follow COTS motor assembly instructions exactly	Low
		Voids/cracks in the propellant			
		Closure failure			
Rocket deviates from planned flight path, achieves lower altitude or hits personnel	Liftoff, Powered ascent	Unstable flight after rail exit	Low, simulation and flight test	Simulated >1.5 body calibers of stability at rail exit	Low
		Launch Tower breaks between ignition and rail exit		Flight test had stable ascent	
Recovery system deploys prematurely in flight	Powered ascent, Coast	Avionics malfunction	Low, flight tested	Flight test verified avionics assembly	Low
		Shear pins prematurely deploy due to differential drag on rocket body		Subsonic flight reduces chance of shocks near vent holes	
Main parachute deploys at or near apogee, rocket or payload drifts to highway(s)	Apogee	Avionics malfunction	Medium, shear pin problem observed in flight test	Vacuum test, flight test verified avionics	Low
		Shear pins prematurely deploy due to shock from drogue deployment		Changed shear pins to 4x 6-32 instead of 3x 4-40, ground tested	

Recovery system fails to deploy, rocket or payload comes in contact with personnel	Apogee, Drogue Descent, Main descent	Avionics short-circuits and/or power-cycles due to high-acceleration events (burnout, drogue deploy)	Low, power-cycling observed in custom avionics during flight test, but successful recovery during flight test.	Avionics assembly procedures updated	Low
		Avionics not armed properly during prelaunch		Detailed chute-packing procedures	
		Chutes packed improperly		Custom avionics hardware revision	
				Redundant electronics	
Recovery system partially deploys, rocket or payload comes in contact with personnel	Apogee, Drogue Descent, Main descent	Avionics short-circuits and/or power-cycles due to high-acceleration events (burnout, drogue deploy)	Low, power-cycling observed in custom avionics during flight test, but successful recovery during flight test	Avionics assembly procedures updated	Low
		Main chute is not removed from deployment bag during flight		Detailed chute-packing procedures	
				Custom avionics hardware revision	
				Redundant electronics	
Rover deploys prematurely and comes in contact with personnel	Main Descent	Sabot deploys early due to shock loads from BP charge and/or main deployment	Medium, not flight tested	Sabot/rover pulled out by main, more likely to be far away from personnel	Medium to mission, Low to personnel
		Altimeter on rover deploys early due to pressure change from BP charge		Ground deployment testing	
Rocket drifts toward personnel and lands at base camp during nominal descent	Main Descent, Landing	Wind conditions are favorable to bring the rocket towards the landing zone	Low, land organization set up with recovery area away from base camp.	Point rocket away from personnel at launch	Low

Fe55 source within rover (for XRF sensor) is no longer contained inside the rover.	All	Recovery system fails to deploy	Low. Causes are mitigated, as shown above.	NRC-exempt source contained within a lead columnator, which is opened for only a moment during science operations.	Low
		Motor catastrophically fails		Operator of the sensor will carry a sensitive Geiger counter at all times.	
				Sensor is protected by rover body, rover enclosure, sabot, and rocket body.	
				Sensor is far away from the motor within the rocket. Motor failure may cause shock loading but should not directly affect sensor.	
				Should main deployment fail, the main chute is placed to protect it from impact	

E. Assembly, Preflight, and Launch Checklists

Assembly Checklists

Motor case and Fin Can:

1. Assemble the motor according to Aerotech instructions
2. Inspect all parts for defects, and ask the integration lead if any defects are found to verify if they are acceptable.
3. Acquire the motor retention bulkhead.
4. Align and place the bulkhead using the bulkhead alignment jig. The bulkhead may need to be fine-tuned using a hex key inserted into the appropriate holes, and reworked.
5. Attach the bulkhead with 6x, $\frac{3}{8}$ " 8-32 screws.
6. Attach the rail button using a [TBR] $\frac{3}{4}$ ", $\frac{1}{4}$ -20 screw. Lightly tighten.
7. Acquire the welded core section, three fins, and 3 sets of three 1" long, 8-32 screws.
8. Insert a fin into one of the thin slots of the welded core section such that the more swept side of the fin is opposite the lip at the bottom of the core section.
9. Insert, and screw in the 8-32 screws by inserting them through the threaded holes in the slots, passing through the corresponding fin hole in the middle. Tighten the screws extremely well to avoid flutter.
10. Repeat for each fin.
11. Verify that the assembly is rotationally symmetric. This assembly is the **fin core**.

12. Insert the fin core into the motor airframe.
13. Ensure all holes align.
14. Attach a rail button to the fin core using a [TBR] ¼”, ¼-20 pan head screw. Lightly tighten.
15. Secure fin core to motor airframe using 15x, ⅜”, 8-32 screws into the alighted holes. Use a 3/32 hex key. Tighten each screw.
- 16. The motor section is now complete for assembly.**
17. Insert assembled motor and threaded rod,
18. Attach ⅜-16 threaded rod into the top of the motor case
19. Secure threaded rod (with the motor) onto the bulkhead assembly.

Drogue/Fin Can Tube:

Check	Procedure	Materials
	Acquire the drogue webbing (labelled Webbing A). Take the side labelled “Fin Can” and use a 1000lb quick-link to attach it to the U-bolt in the fin-can. Confirm that the quick-link has been tightened with a wrench.	
	Use a 1000lb quick-link to connect the drogue parachute to a 1500lb swivel. Confirm that the quicklink is tightened with a wrench.	
	Use a 1000lb quick-link to connect the other side of the 1500lb swivel to the water knot in the middle of Webbing A and a piece of nomex. Confirm that this quicklink is tightened with a wrench.	
	Infinity wrap the webbing on both sides of the drogue parachute.	
	Individually tape both infinity wraps with one wrap of tape each.	
	Carefully fold the drogue parachute and place it, the webbing, and the shroud lines on top of the Nomex.	
	Carefully wrap everything (webbing, drogue, shroud lines, etc.) with Nomex. Make sure that nothing is exposed except the short length of webbing to attach to the AV Bay.	
	Slide this assembly inside the motor section. Be cognizant of how tight the fit is, and redo it if the integration lead says so. Ensure that no part of the nomex wrap comes undone.	
	Take the side of webbing that is labeled “AV Bay” and use a 1000lb quick-link to attach it to appropriate side of the Avionics Bay. The sides should be labeled but, if not, the Drogue side has smaller charge canisters than the Main side. Confirm that the quick-link is tightened with a wrench.	
	Use alignment markers to determine proper AV Bay location relative to fin can tube.	
	Slide the Avionics bay into the motor section, insert shear pins and tape over them.	

Nose Cone:

Check	Procedure	Materials
	Determine the appropriate amount of ballast using the simulation.	
	Attach the nose cone tip and ¼-20 threaded rod to each other, and insert the rod into the top of the nose cone.	
	Take appropriate amount of ballast and slide onto the ¼-20 threaded rod for the nose cone from the inside. Stack the ballast pieces from smallest to largest, with the smallest going further inside the nose cone.	
	Place the nose cone bulkhead on the bottom of the stack, inserting the threaded rod through the center.	
	Attach a ¼-20 nut w/ ***	
	Screw on tip of nose cone, making sure that the tip and ballast stay axially aligned.	

Payload/Recovery Tube:

Check	Procedure	Materials
	Pack the main parachute into the deployment bag. (See Main Parachute Checklist)	
	Use a 1000lb quick-link to attach the ends of the shroud lines to a 1500lb swivel. Check the quick-link with a wrench.	
	Use another 1000lb quick-link to connect the other side of the swivel to the knot in Webbing B labelled “Main Parachute”. It is the knot closer to the end labelled “Nose Cone”. Check the quick-link with a wrench.	
	Quick-link (1000lb) the not short length of red webbing attached to the deployment bag to the “Nose Cone” side of the purple webbing. The long length of red webbing is actually labeled “Not the short side.” This quick-link does not need to be secured with a wrench. In fact, you will need to undo this quick-link later to attach it to something else.	
	Use another 1000lb quick-link to secure the sabot onto the other water knot (the water knot closest to the end of webbing labeled “AV Bay.” Tighten with a wrench.	
	Infinity wrap all sections of webbing (AV Bay → Sabot, Sabot → Main, and Main → Nose Cone) and secure each with a small amount of tape (one wrap is sufficient). You will need to leave enough webbing unwrapped in order for it to pass alongside the groove of the sabot. There is a bit of Duct tape on the webbing that is labelled “You shall not pass.” This will help you determine how much webbing should be free to run alongside the Sabot.	
	Remove tape from deployment bag.	
	Feed the deployment bag (red webbing end first), webbing, and sabot (eye nut side first) from the av bay side to the nose cone side of the tube. The deployment bag should be closer to the Nose Cone than the Sabot.	

		Now, undo the quick-link from Step 3 and re-attach it to the U-bolt inside the nose cone. BOTH the deployment bag and the purple webbing should be attached to this quick-link. Secure the quick-link with a wrench.	
		Align the nose cone and slide it into the payload-recovery tube. Secure the nosecone with 3 shear pins. Tape over the shear pins.	
		Moving to the AV Bay side of the Payload/Recovery tube, use a 1000lb quick-link to secure the end of the Purple webbing and a piece of nomex to the AV Bay. Check your quicklink with a wrench.	
		Burrito the purple webbing below the sabot with nomex and push this webbing into the tube.	
		Align the Avionics Bay and the Payload/Recovery tube and slide the tubes together.	
		Put 3 8-32's in the 3 attachment holes	

Preflight Checklist

Weight and Balance:

Check	Procedure	Materials
	Verify rocket's total mass against OpenRocket model	Assembled rocket Scale Laptop with OpenRocket model
	Verify rocket's center of gravity location against OpenRocket model	
	Adjust simulation if necessary	
	Adjust ballast if necessary to achieve safe stability margin	

Judge's Inspection:

	Procedure	
	Check that the rocket slides on the rail buttons	
	Inspect fins and other external structures	
	Complete the payload weighing	
	Obtain permission to approach the launch pad	Assembled rocket IREC judges

Put rocket on launch rail:

1. Tip rail down

2. Slide rocket onto rail
3. Raise rail to vertical
4. Lock rail

Materials:

Assembled rocket

Launch rail

Avionics startup:

1. Cameras:
 - a. Turn on and start recording both axial cameras
 - b. Turn on and start recording radial camera
 - c. Install radial camera into slot and secure in place
 - d. Remove lens caps from all cameras
2. Flight Computers:
 - a. Turn on Pyxida ground station
 - b. Turn on TeleMetrum ground station
 - c. Remove avionics switchband cover
 - d. Turn all four switches to 220 position
 - e. Listen for stratologger beeps. Confirm
 - i. Good battery voltage.
 - ii. Main deployment altitude
 - iii. Pyro channel continuity
 - f. Check telemetry on Pyxida ground station:
 - i. GPS lock near 38° 48" N, 109° 56" W
 - ii. Continuity on pyro channels
 - iii. Barometric altitude close to 0 ± 20 m
 - g. Check telemetry on TeleMetrum ground station:
 - i. GPS lock near 38° 48" N, 109° 56" W
 - ii. Continuity on pyro channels
 - iii. Barometric altitude close to 0 ± 20 m
 - h. Reinstall avionics switchband cover

Materials:

Assembled rocket

Small Phillips screwdriver

Small slotted screwdriver

Laptop with ground station software

Pyxida ground receiver

TeleMetrum ground receiver

Propulsion setup:

1. Everyone step away from launch pad except Team Lead, Safety Officer, and Propulsion Operator
2. Install igniter:
 - a. Remove motor cover
 - b. Insert igniter on stick into the motor throat
 - c. Replace the motor cover, with the igniter wires sticking out
3. Connect the igniter wires to the launch control system

Materials:

Igniter on stick

Motor cover

Launch Checklist

- 1) Check with IREC officials for launch clearance
- 2) Ensure all avionics are properly armed and communicating
- 3) Ensure all personnel are clear of launch site
- 4) Ensure sky is clear of any planes or other obstructions
- 5) Commence launch with on-site launch equipment
- 6) If an ignition failure occurs, wait a minimum of 60 seconds and obtain permission from IREC official before approaching the pad.

F. Engineering Drawings

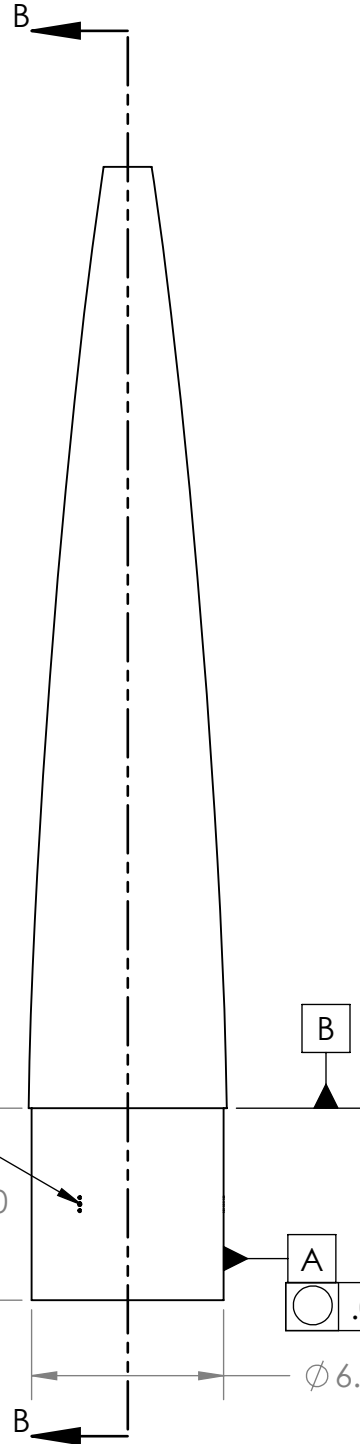
This appendix contains relevant engineering drawings for the structure of the rocket. The following drawings are included, in this order: Nosecone, Payload Tube, Av Bay Switchband, Av Bay Coupler, and Fin Can Airframe. Drawings are given in the subsequent pages.

4

1

3

E

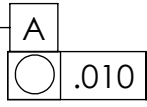


3X HOLE PATTERN A
 3.00 FROM B
 90, 210, 330 deg

PLY TABLE

PLY #	MATERIAL
1	S-GLASS PLAIN WEAVE
2	S-GLASS PLAIN WEAVE
3	S-GLASS PLAIN WEAVE
4	S-GLASS PLAIN WEAVE
5	S-GLASS PLAIN WEAVE

6.00



A
 .010

Ø 6.00

SIDE VIEW

A

A

UNLESS OTHERWISE SPECIFIED:
 DIMENSIONS ARE IN INCHES
 DEFAULT TOLERANCES:

X.X => ±0.1
 X.XX => ±0.03
 X.XXX => ±0.005

TITLE:

MATERIAL

SIZE

DWG. NO.

REV

FINISH

A ST-NC-001

SOLIDWORKS Educational Product. For Instructional Use Only

DO NOT SCALE DRAWING

SCALE: 1:6 WEIGHT:

SHEET 1 OF 2

0

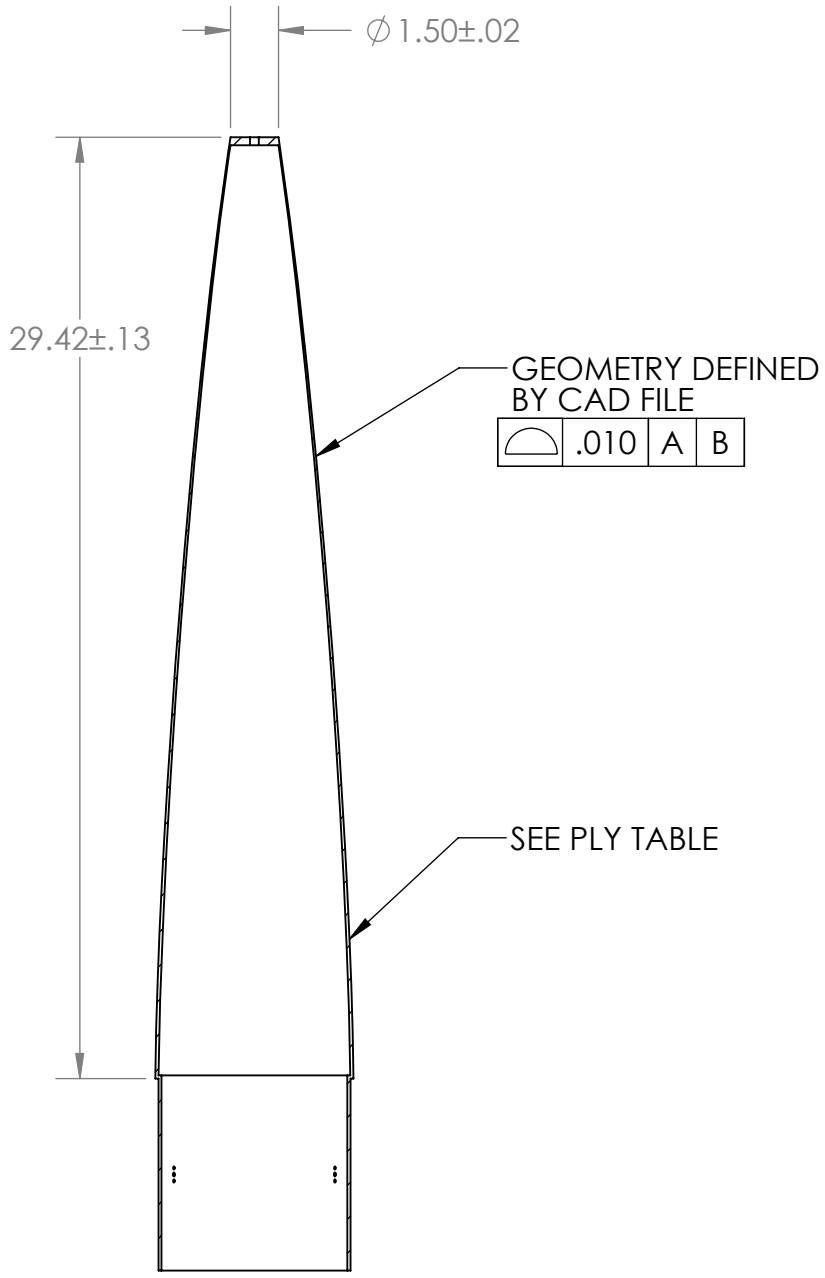
1

4

1

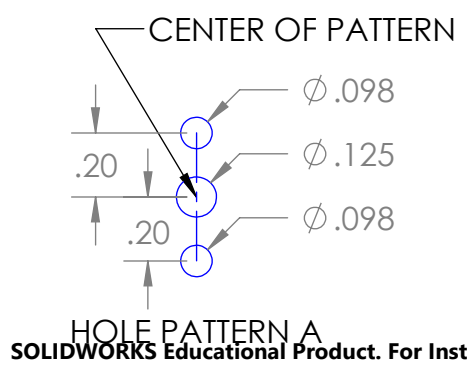
3

E



A

A



SECTION B-B

UNLESS OTHERWISE SPECIFIED: DIMENSIONS ARE IN INCHES DEFAULT TOLERANCES: X.X => ±0.1 X.XX => ±0.03 X.XXX => ±0.005		TITLE:	
MATERIAL	SIZE	DWG. NO.	REV
FINISH	A	ST-NC-001	
DO NOT SCALE DRAWING		SCALE: 1:6	WEIGHT: SHEET 2 OF 2

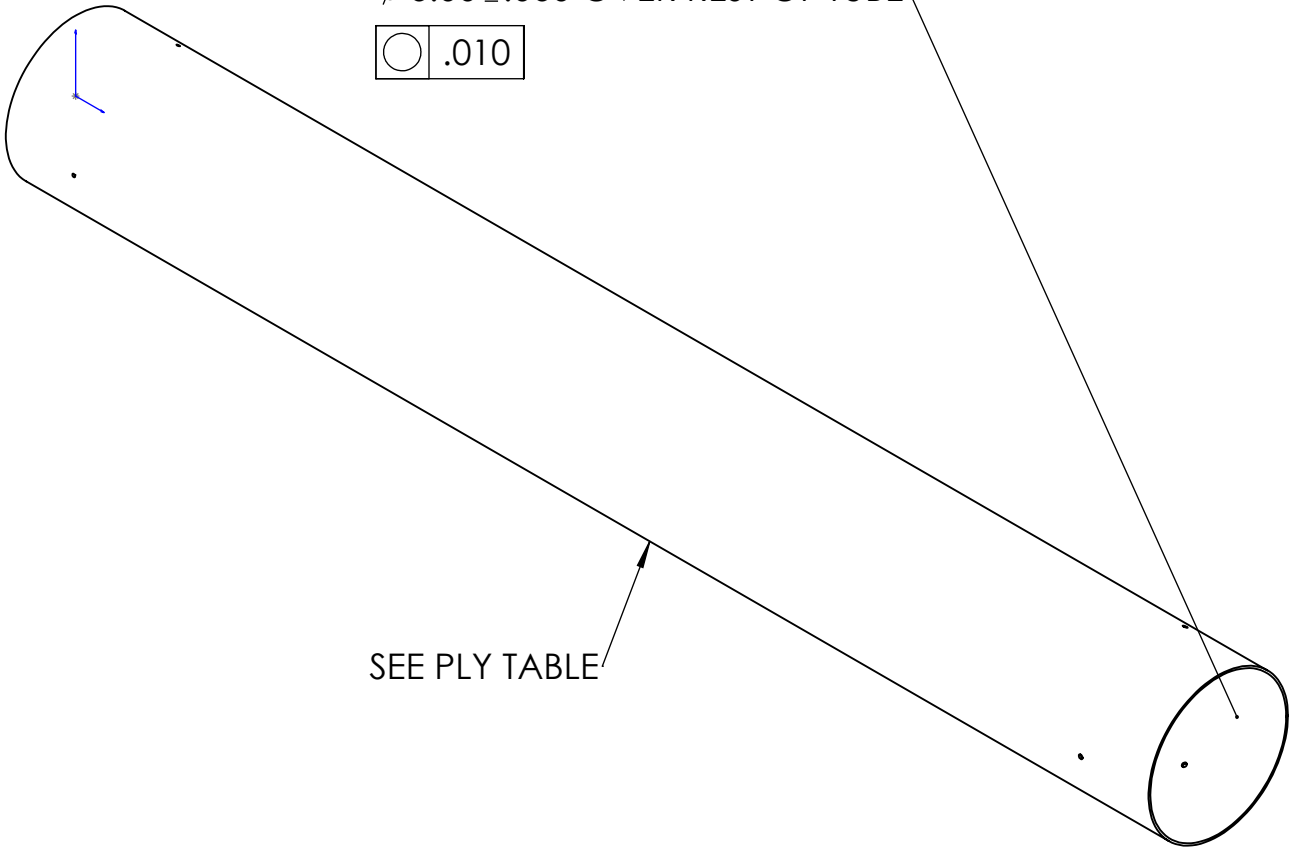
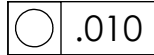
3

1

4

1

∅ 6.00 ± .010 AT LEAST 6IN FROM EITHER END
∅ 6.00 ± .060 OVER REST OF TUBE



3

E

SEE PLY TABLE

PLY TABLE

PLY #	MATERIAL
1	S-GLASS PLAIN WEAVE
2	S-GLASS PLAIN WEAVE
3	S-GLASS PLAIN WEAVE
4	S-GLASS PLAIN WEAVE
5	S-GLASS PLAIN WEAVE

A

A

UNLESS OTHERWISE SPECIFIED:
DIMENSIONS ARE IN INCHES
DEFAULT TOLERANCES:

X.X => ±0.1
X.XX => ±0.03
X.XXX => ±0.005

TITLE:

Payload Tube

MATERIAL
S-Glass Fiberglass

SIZE
A

DWG. NO.
ST-PY-001

REV

SOLIDWORKS Educational Product. For Instructional Use Only

DO NOT SCALE DRAWING

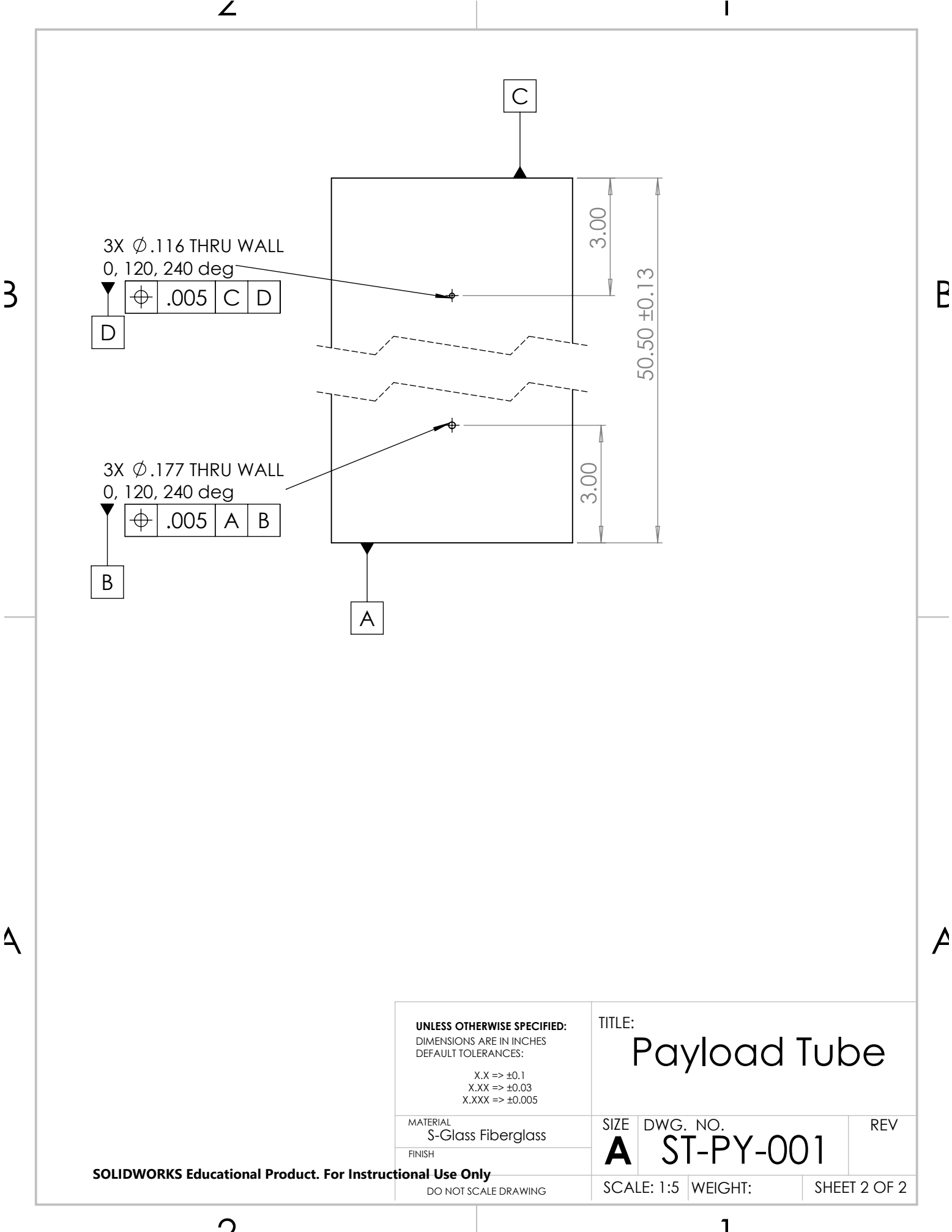
SCALE: 1:5

WEIGHT:

SHEET 1 OF 2

3

1

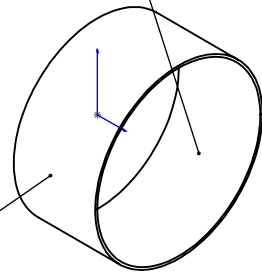


4

1

Ø 6.00 ± .010 ID

○ .010

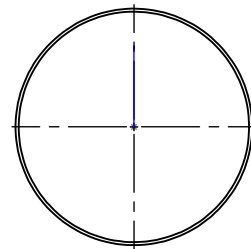
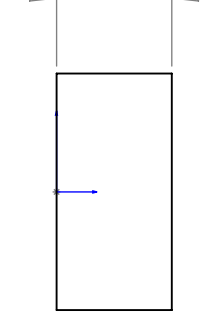


SEE PLY TABLE

3

E

3.00 ± 0.13



PLY TABLE

PLY #	MATERIAL
1	S-GLASS PLAIN WEAVE
2	S-GLASS PLAIN WEAVE
3	S-GLASS PLAIN WEAVE
4	S-GLASS PLAIN WEAVE
5	S-GLASS PLAIN WEAVE

A

A

UNLESS OTHERWISE SPECIFIED:
DIMENSIONS ARE IN INCHES
DEFAULT TOLERANCES:

X.X => ±0.1
X.XX => ±0.03
X.XXX => ±0.005

TITLE:

Av Bay
Switchband

MATERIAL
S-Glass Fiberglass

SIZE DWG. NO.

A ST-AB-001

REV

SOLIDWORKS Educational Product. For Instructional Use Only

DO NOT SCALE DRAWING

SCALE: 1:5 WEIGHT:

SHEET 1 OF 1

2

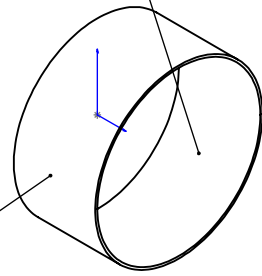
1

4

1

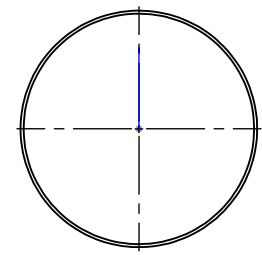
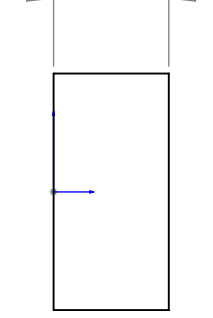
Ø 6.00 ± .010 ID

○ .010



SEE PLY TABLE

3.00 ± 0.13



3

E

PLY TABLE

PLY #	MATERIAL
1	S-GLASS PLAIN WEAVE
2	S-GLASS PLAIN WEAVE
3	S-GLASS PLAIN WEAVE
4	S-GLASS PLAIN WEAVE
5	S-GLASS PLAIN WEAVE

A

A

UNLESS OTHERWISE SPECIFIED:
DIMENSIONS ARE IN INCHES
DEFAULT TOLERANCES:

X.X => ±0.1
X.XX => ±0.03
X.XXX => ±0.005

TITLE:

Av Bay
Switchband

MATERIAL
S-Glass Fiberglass

SIZE
A

DWG. NO.
ST-AB-001

REV

SOLIDWORKS Educational Product. For Instructional Use Only

DO NOT SCALE DRAWING

SCALE: 1:5


WEIGHT:

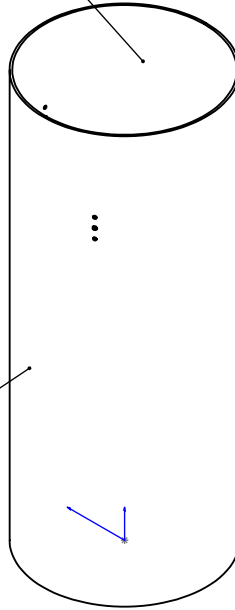
SHEET 1 OF 1

2

1

$\varnothing 6.00 \pm .010$ AT LEAST 6IN FROM EITHER END
 $\varnothing 6.00 \pm .060$ OVER REST OF TUBE

	.010
---	------



SEE PLY TABLE

PLY TABLE

PLY #	MATERIAL
1	S-GLASS PLAIN WEAVE
2	S-GLASS PLAIN WEAVE
3	S-GLASS PLAIN WEAVE
4	S-GLASS PLAIN WEAVE
5	S-GLASS PLAIN WEAVE

UNLESS OTHERWISE SPECIFIED:
 DIMENSIONS ARE IN INCHES
 DEFAULT TOLERANCES:

X.X => ± 0.1
 X.XX => ± 0.03
 X.XXX => ± 0.005

MATERIAL
 S-Glass Fiberglass

FINISH

TITLE:

Av Bay Coupler

SIZE
A

DWG. NO.

ST-AB-002

REV

SOLIDWORKS Educational Product. For Instructional Use Only

DO NOT SCALE DRAWING

SCALE: 1:5

WEIGHT:

SHEET 1 OF 2

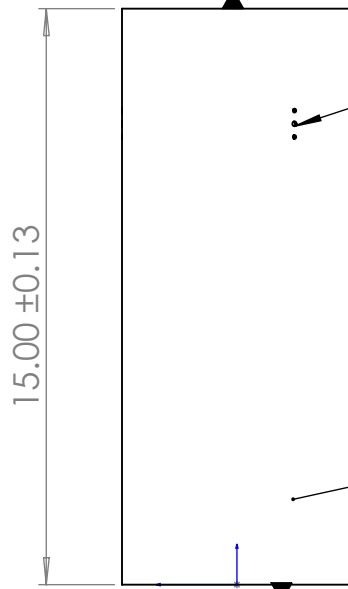
4

1

3

B

A



3X HOLE PATTERN A
 3.00" FROM A
 30, 150, 270

\varnothing	.005	A
---------------	------	---

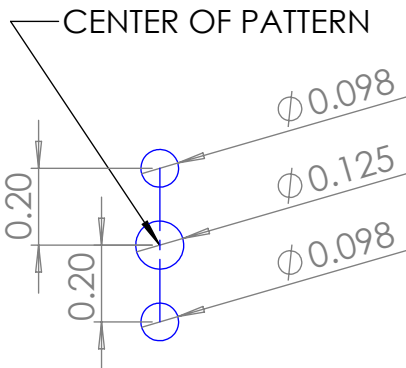
3X \varnothing .116 THRU WALL
 3.00" FROM A
 45, 150, 270

\varnothing	.005	B
---------------	------	---

B

A

A



HOLE PATTERN A
 SOLIDWORKS Educational Product. For Instructional Use Only

UNLESS OTHERWISE SPECIFIED:
 DIMENSIONS ARE IN INCHES
 DEFAULT TOLERANCES:

X.X => ±0.1
 X.XX => ±0.03
 X.XXX => ±0.005

TITLE:

Av Bay Coupler

MATERIAL
 S-Glass Fiberglass

SIZE DWG. NO.

A ST-AB-002

REV

FINISH

SCALE: 1:5

WEIGHT:

SHEET 2 OF 2

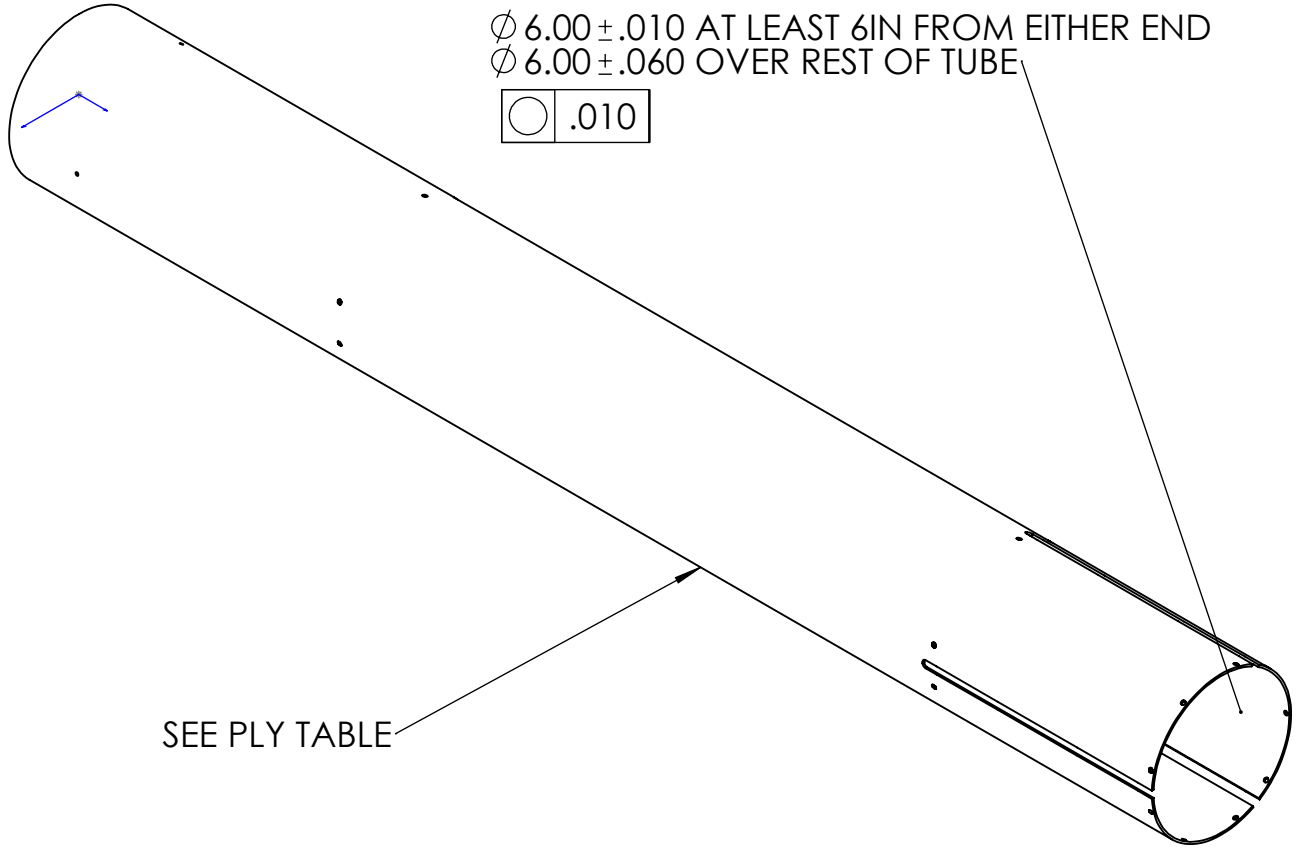
DO NOT SCALE DRAWING

3

1

4

1



$\varnothing 6.00 \pm .010$ AT LEAST 6IN FROM EITHER END
 $\varnothing 6.00 \pm .060$ OVER REST OF TUBE

○	.010
---	------

SEE PLY TABLE

PLY TABLE

PLY #	MATERIAL
1	S-GLASS PLAIN WEAVE
2	S-GLASS PLAIN WEAVE
3	S-GLASS PLAIN WEAVE
4	S-GLASS PLAIN WEAVE
5	S-GLASS PLAIN WEAVE

UNLESS OTHERWISE SPECIFIED:
 DIMENSIONS ARE IN INCHES
 DEFAULT TOLERANCES:

X.X => ±0.1
 X.XX => ±0.03
 X.XXX => ±0.005

MATERIAL
 S-Glass Fiberglass

FINISH

TITLE:

Fin Can Airframe

SIZE DWG. NO.

A ST-FC-001

REV

SOLIDWORKS Educational Product. For Instructional Use Only

DO NOT SCALE DRAWING

SCALE: 1:5 WEIGHT:

SHEET 1 OF 2

3

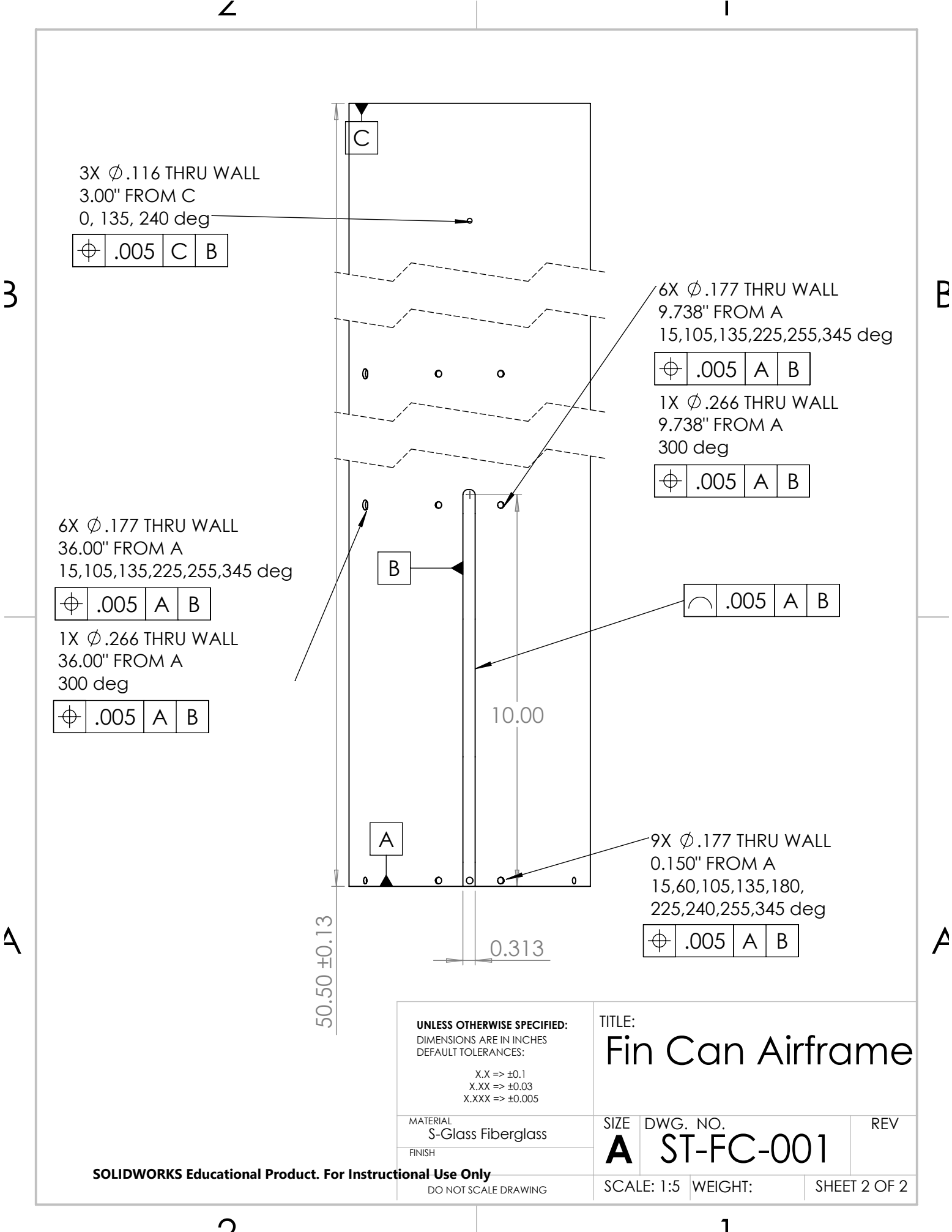
1

A

A

3

3



Acknowledgments

The Team would like to thank their faculty advisor Professor Warren Hoburg for his support throughout the design, manufacturing, and testing of Project Raziell. The Team would also like to thank the MIT Department of Aeronautics and Astronautics for providing lab space, tools, and resources. The Team is grateful for the support of many individuals within the MIT Department of Aeronautics and Astronautics, including Anthony Zolnik, Todd Neumann, Todd Billings, and David Robertson for their reliable technical and administrative assistance. In addition, the Team would like to thank the Edgerton Center Administrative Officer Sandra Lipnoski for her continued help in management of purchasing and finances. Lastly, the Team would like to thank their sponsors for their financial support in making Project Raziell possible: MIT Edgerton Center, MIT Department of Aeronautics and Astronautics, Northrop Grumman Corporation, Arconic, A&M Tool & Die Company, Asana, Blue Origin, OSH Park, MIT Department of Mechanical Engineering, and Markforged.

References

- [1] Crowell, G. A., "The Descriptive Geometry of Nose Cones," 1996.
- [2] Perkins, E. W., Jorgenson, L. H., and Sommer, S. C., *Investigation of the Drag of Various Axially Symmetric Nose Shapes of Fineness Ratio 3 for Mach Numbers from 1.24 to 7.4*.
- [3] Crowell, G. A., "The Descriptive Geometry of Nose Cones," 1996.
- [4] Alvero, V., and Toft, H. O., "Deciding Which Nose Cone Shape To Use For A High-Altitude Rocket," *Peak of Flight*, Oct. 2014.
- [5] Perkins, E. W., Jorgenson, L. H., and Sommer, S. C., *Investigation of the Drag of Various Axially Symmetric Nose Shapes of Fineness Ratio 3 for Mach Numbers from 1.24 to 7.4*.
- [6] Perkins, E. W., Jorgenson, L. H., and Sommer, S. C., *Investigation of the Drag of Various Axially Symmetric Nose Shapes of Fineness Ratio 3 for Mach Numbers from 1.24 to 7.4*.
- [7] Seiff, A., and Sandahl, C. A., *The Effect of Nose Shape on the Drag of Bodies of Revolution at Zero Angle of Attack*.
- [8] Nakka, R. (2017, April 17). Parachute Design and Construction. Retrieved May 14, 2017, from <https://www.nakka-rocketry.net/paracon.html>
- [9] Bixby, H., Ewing, E., and Knacke, T. (1978). *Recovery System Design Guide*. Gardena, California: Irvin Industries Inc.
- [10] Shear Pins. (n.d.). Retrieved May 26, 2017, from http://www.telerover.com/rockets/L3/HPR_ShearPinTests.pdf. Originally published on RocketMaterials.org
- [11] Black Powder Calculator. (n.d.). Retrieved May 28, 2017, from <http://www.chmara.com/bt/rocketry/bpcalc.html>.